Mem. Descr. Carta Geol. d'It.
XLIV (2004), pp.29-56
7 figg.

Structure of the lithosphere-asthenosphere and volcanism in the Tyrrhenian Sea and surroundings
Struttura della litosfera-astenosfera e vulcanismo nel Mar Tirreno e regioni adiacenti

PANZA G.F. (*), PONTEVIVO A. (**), SARAÒ A. (***),
AOUDIA A. (****), PECCERILLO A. (*****)

ABSTRACT - The Italian peninsula and the Tyrrhenian Sea are some of the geologically most complex regions on Earth. Such a complexity is expressed by large lateral and vertical variations of the physical properties as inferred from the lithosphere-asthenosphere structure and by the wide varieties of Plio-Quaternary magmatic rocks ranging from tholeiitic to calcalkaline to sodium- and potassium-alkaline and ultra-alkaline compositions.
The integration of geophysical, petrological and geochemical data allows us to recognise various sectors in the Tyrrhenian Sea and surrounding areas and compare different volcanic complexes in order to better constrain the regional geodynamics. A thin crust overlying a soft mantle (10% of partial melting) is typical of the back arc volcanism of the central Tyrrhenian Sea (MAGNAGHI, VAVILOV & MARSILI) where tholeiitic rocks dominate. Similar lithosphere-asthenosphere structure is observed for Ustica, Vulture and Etna volcanoes where the geochemical signatures could be related to the contamination of the side intraplate mantle by material coming from either ancient or active roll-back. The lithosphere-asthenosphere structure and geochemical-isotopic composition do not change significantly when we move to the Stromboli-Campanian volcanoes, where we identify a well developed low-velocity layer, about 10-15 km thick, below a thin lid, overlain by a thin continental crust. The geochemical signature of the nearby Ischia volcano is characteristic of the Campanian sector and the relative lithosphere-asthenosphere structure may likely represent a transition to the back arc volcanism sector acting in the central Tyrrhenian. The difference in terms of structure beneath Stromboli and the nearby Vulcano and Lipari is confirmed by different geochemical signatures. The affinity between Vulcano, Lipari and Etna could be explained by their common position along the Tindari-Letoianni-Malta fault zone. A low velocity mantle wedge, just below the Moho, is present in all the regions related to the inactive recent volcanoes (Amiata, Vulsini, & Cimino, Vico, Sabatini, Albani Hills) in the Tuscany and Roman regions. A very thick rigid body is found in the upper mantle beneath the Ernici-Roccamonfina province that exhibits very distinct geochemical and isotopic compositions when compared with the Roman province.

KEY WORDS: lithosphere-asthenosphere system, geochemical-isotopic composition, Italian volcanic provinces, magma sources.

RIASSUNTO - La penisola italiana ed il Mar Tirreno sono alcune tra le regioni più complesse dal punto di vista geologico. Tale complessità è resa evidente da ampie variazioni verticali e laterali nelle proprietà fisiche della struttura litosfera-astenosfera e dalla grande varietà di rocce magmatiche del

(*) Dipartimento di Scienze della Terra, Università degli Studi di Trieste, Italy. (panza@dst.univ.trieste.it, aoudia)
The Abdus Salam International Centre for Theoretical Physics, SAND Group, Trieste, Italy.
(**) Dipartimento di Scienze della Terra, Università degli Studi di Trieste, Italy. (panza@dst.univ.trieste.it, aoudia)
now at the Geological Institute, University of Copenhagen, Denmark. (antonella@geo.geol.ku.dk)
(***) Dipartimento di Scienze della Terra, Università degli Studi di Trieste, Italy. (panza@dst.univ.trieste.it, aoudia.)
now at Osservatorio Vesuviano – INGV, Naples, Italy. (sarao@ov.ingv.it)
(****) Dipartimento di Scienze della Terra, Università degli Studi di Trieste, Italy. (panza@dst.univ.trieste.it, aoudia.)
The Abdus Salam International Centre for Theoretical Physics, SAND Group, Trieste, Italy.
(*****) Dipartimento di Scienze della Terra, Università degli Studi di Perugia, Italy. (pecceang@unipg.it)

periodo Plio-Quaternario, la cui composizione varia da toleitica a calcalcalina, da sodio- e potassio-alcalina ad ultra-alcalina.
L'analisi contestuale di dati geofisici, petrologici e geochimici ha permesso di riconoscere vari settori del mar Tirreno e delle aree circostanti e di mettere a confronto diversi complessi vulcanici con lo scopo di porre vincoli attendibili ai processi geodinamici regionali. La presenza di una crosta sottile che sovrasta un mantello soffice (10% di fusione parziale) è tipica del vulcanismo di retro-arco presente nel Tirreno centrale, dove predominano le rocce toleitiche. Una struttura litosfera-astenosfera simile è stata osservata in corrispondenza dei vulcani Ustica, Vulture ed Etna, dove le caratteristiche geochimiche possono essere legate alla contaminazione del mantello da parte di materiale derivante da processi di roll-back recenti o passati. La struttura litosfera-astenosfera e la composizione geochimica-isotopica non cambiano in modo significativo se si considerano Stromboli e i vulcani campani dove uno strato a bassa velocità ben sviluppato, dello spessore di 10-15 km, è presente sotto un sottile lid, sovrastato da una sottile crosta continentale. L'impronta geochimica del vicino vulcano di Ischia è caratteristica del settore campano e la relativa struttura litosfera-astenosfera può verosimilmente rappresentare una transizione al settore caratterizzato dal vulcanismo di retro-arco che è presente nel Tirreno centrale. La differenza, in termini di struttura, tra lo Stromboli ed i vicini Vulcano e Lipari è confermata dalle diverse caratteristiche geochimiche. L'affinità tra Vulcano, Lipari ed Etna può, invece, essere spiegata dalla loro comune posizione lungo la zona di faglia Tindari-Letoianni-Malta. Nella regione Toscana e nella provincia Romana, il mantello, a bassa velocità, affiora subito sotto la Moho in tutte le regioni in cui sono presenti vulcani recenti inattivi (Amiata, Vulsini, Cimino, Vico, Sabatini, Albani, Hills). Nel mantello superiore sotto la zona Ernici-Roccamorfina è stato identificato un corpo rigido e molto spesso che presenta composizioni geochimiche ed isotopiche ben distinte se paragonate con la provincia Romana.

PAROLE CHIAVE: sistema litosfera-astenosfera, composizione geochimica-isotopica, provincie vulcaniche italiane, sorgenti dei magmi

1. - INTRODUCTION

Volcanism is controlled by the lithosphere structure and architecture (e.g. MCNUTT, 1998; ANDERSON, 2000). The Italian peninsula and the Tyrrhenian Sea are some of the geologically most complex regions on Earth. Such a complexity is expressed by the strong heterogeneities of the crust-mantle system and the wide varieties of Plio-Quaternary magmatic rocks (e.g. PECCERILLO & PANZA, 1999). This setting is the result of the complex geodynamic evolution, of the Mediterranean during the Neogene and Quaternary times (e.g. DOGLIONI *et alii*, 1999). This generated a mosaic of compositionally and structurally distinct mantle domains that have undergone different evolutionary histories in terms of compositional and structural modifications.

The geodynamic evolution of the Mediterranean can be hardly unravelled when making use of models based on mono-disciplinary investigations. This is due to the complexity of the study area and to the intrinsic non-uniqueness of the inverse problem that is at the base of any geological model. In this paper we supply geophysical, petrological and geochemical data relative to different magmatic provinces recognised in Peninsular Italy and in the Tyrrhenian Sea. We combine the different datasets in order to better understand the genesis of the recent volcanism. Tying together geophysics, petrology and geochemistry we recognise various sectors in the Tyrrhenian Sea and surrounding areas and compare different volcanic complexes in order to better constrain the regional geodynamics.

2. - GEOPHYSICAL DATA AND METHOD

We determine the thickness and the vertical velocity distribution of the shear waves in the lithospheric layers for the area under investigation, represented in figure 1, using the surface-wave tomography regional study made by PONTEVIVO & PANZA (2002) and, where pertinent, the large-scale one by PASYANOS *et alii* (2001).

The available surface waves dispersion curves at regional scale (PONTEVIVO & PANZA, 2002; PANZA *et alii*, 2003), have been used to obtain tomography maps using the two-dimensional tomography algorithm developed by DITMAR & YANOVSKAYA (1987), YANOVSKAYA & DITMAR (1990). The lateral resolving power of the available dispersion data is of about 200 km (PONTEVIVO & PANZA, 2002); however the availability of a priori independent geological and geophysical information about the uppermost part of the crust improves the lateral resolving power and justifies the choice to perform the non-linear inversion of dispersion curves averaged over cells of a 1°x1° grid (PANZA *et alii*, 2003). Each cell of the grid is characterised by average dispersion curves of group velocity, $V_g(T)$ (in the period range of 10-35 s), and of phase velocity, $V_{ph}(T)$ (in the period range of 25-100 s). Each mean velocity is the average of the values read from the relevant tomography maps of PONTEVIVO & PANZA (2002) at the four nodes of each 1°x1° cell. The dispersion relations computed in such a way are listed in table 1. In the same table are shown the errors considered in the inversion, at each period. Following PANZA *et alii* (2003), each single point error (ρ_g, ρ_{ph}) associated to group and phase velocity values of a cell, is the quadratic sum of the measurement error (ρ'_g, ρ'_{ph}) and of the standard deviation (σ_g, σ_{ph}) of the average cellular velocities ($V_g(T)$, $V_{ph}(T)$).

At each period, the measurement error associated to the group velocity is estimated from the difference

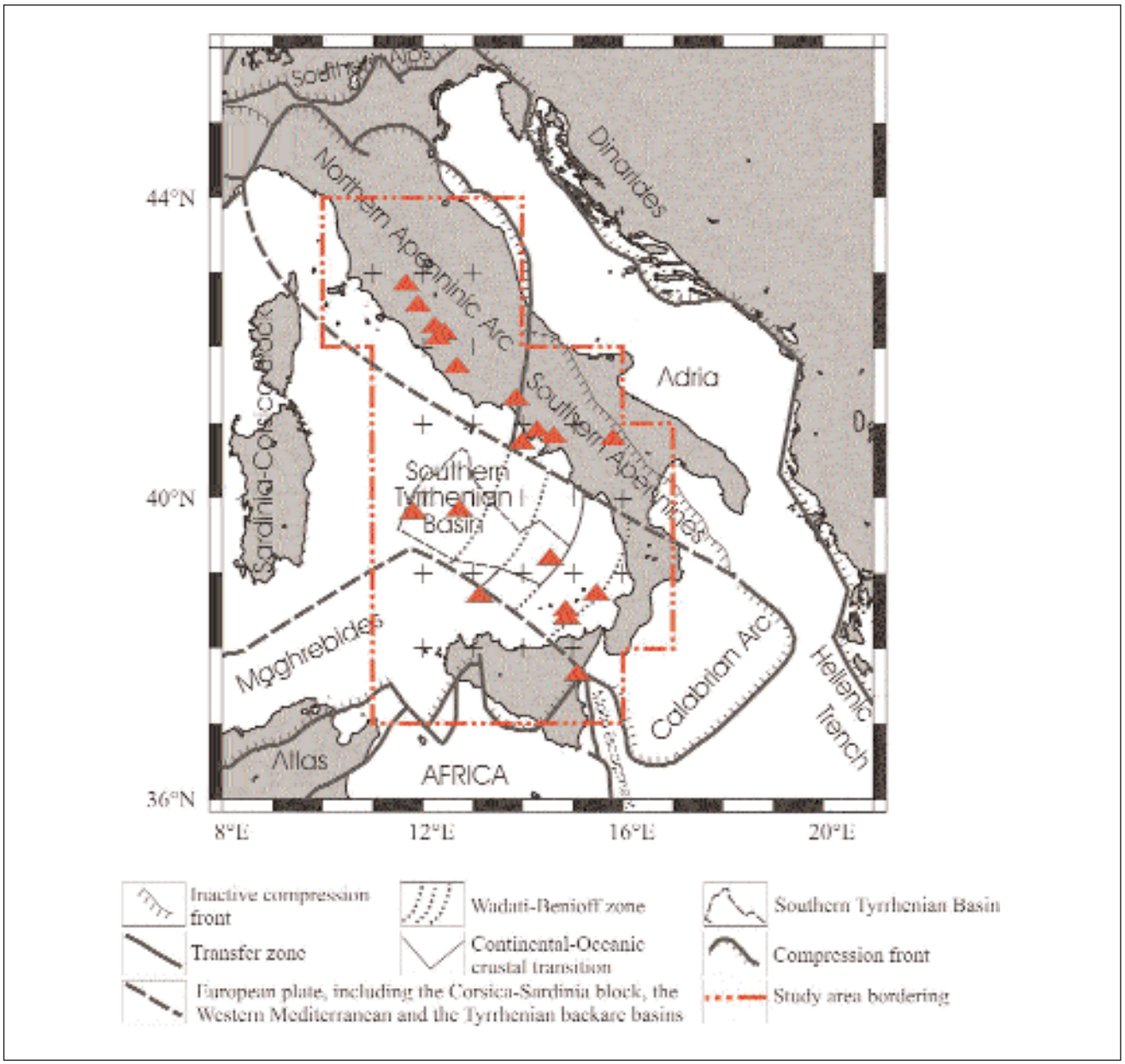

Fig. 1. - *Structural and kinematic sketch of Italy and surrounding areas, modified from* MELETTI *et alii* (2000). *The recent (active and not active) volcanoes in the study area (see the legend) are indicated by triangles.*

in the group velocity values determined along similar paths crossing similar areas, and is considered to be the same, ρ'_g, in all the cells well covered by the source-receiver paths. For the cells with a low path-coverage, the assumed error in the inversion is $2\rho'_g$. The measurement error associated to the phase velocity, ρ'_{ph}, is fixed accordingly to typical values published in the literature (BISWAS & KNOPOFF, 1974; CAPUTO *et alii*, 1976) for cells with a good path-coverage, and it is $2\rho'_{ph}$ elsewhere.

The parametrization of the structure to be inverted is chosen taking into account the resolving power of the data (KNOPOFF & PANZA, 1977; PANZA 1981) and relevant petrological information (e.g. RINGWOOD, 1966; GRAHAM, 1970; AHRENS, 1973; BOTTINGA & STEINMETZ, 1979; DELLA VEDOVA *et alii*, 1991). In such a way we have fixed the upper limit of V_S, for the sub-Moho mantle, at 4.9 km/s, and the lower limit of V_s at 4.0 km/s for the asthenosphere at depths greater than about 60 km. Average models of the lower crust and of the upper mantle are retrieved by the non-linear inversion method called Hedgehog (VALYUS *et alii*, 1969; VALYUS, 1972; KNOPOFF, 1972; PANZA, 1981). Following this procedure, the structure is modeled as a stack of N homogeneous isotropic layers in the elastic approximation, and each layer is

Tab. 1 - *Group (Vg) and phase (Vph) velocity values at different periods (from 10 s to 35 s and from 25 s to 100 s, respectively) with the single point error (g, ph) and the r.m.s. values for each cell. All phase velocities have been corrected for sphericity following* BOLT & DORMAN (1961).

	Cell c0 (10.5; 43.5)				**Cell c1 (11.5; 43.5)**				**Cell c2 (12.5; 43.5)**				**Cell c3 (13.5; 43.5)**				**Cell b0 (10.5; 42.5)**			
Period	V_g	ρ_g	V_{ph}	ρ_{ph}	V_g	ρ_g	V_{ph}	ρ_{ph}	V_g	ρ_g	V_{ph}	ρ_{ph}	V_g	ρ_g	V_{ph}	ρ_{ph}	V_g	ρ_g	V_{ph}	ρ_{ph}
(s)	(km/s)	(km/s)	(km/s)	(km/s)	(km/s)	(km/s)	(km/s)	(km/s)	(km/s)	(km/s)	(km/s)	(km/s)	(km/s)	(km/s)	(km/s)	(km/s)	(km/s)	(km/s)	(km/s)	(km/s)
10	1.96	0.20			2.01	0.10			2.09	0.10			2.18	0.11			2.15	0.21		
15	2.17	0.16			2.13	0.09			2.16	0.08			2.22	0.10			2.52	0.20		
20	2.43	0.16			2.38	0.08			3.38	0.07			2.42	0.08			2.81	0.19		
25	2.66	0.16	3.53	0.11	2.61	0.07	3.50	0.11	2.61	0.07	3.51	0.11	2.63	0.08	3.56	0.11	2.99	0.18	3.54	0.11
30	2.96	0.17	3.61	0.09	2.89	0.09	3.60	0.09	2.86	0.08	3.62	0.09	2.85	0.08	3.67	0.09	3.24	0.18	3.63	0.09
35	3.14	0.33	3.67	0.08	3.11	0.17	3.67	0.08	3.06	0.16	3.69	0.08	3.01	0.16	3.73	0.08	3.42	0.33	3.68	0.08
50			3.81	0.06			3.81	0.06			3.83	0.06			3.86	0.06			3.82	0.06
80			3.94	0.06			3.94	0.06			3.95	0.06			3.95	0.06			3.92	0.06
100			3.97	0.06			3.97	0.06			3.97	0.06			3.98	0.06			3.97	0.06
r.m.s.		0.12		0.055		0.07		0.055		0.07		0.055		0.07		0.055		0.13		0.055
	Cell b1 (11.5; 42.5)				**Cell b2 (12.5; 42.5)**				**Cell b3 (13.5; 42.5)**				**Cell a1 (11.5; 41.5)**				**Cell a2 (12.5; 41.5)**			
Period	V_g	ρ_g	V_{ph}	ρ_{ph}	V_g	ρ_g	V_{ph}	ρ_{ph}	V_g	ρ_g	V_{ph}	ρ_{ph}	V_g	ρ_g	V_{ph}	ρ_{ph}	V_g	ρ_g	V_{ph}	ρ_{ph}
(s)	(km/s)	(km/s)	(km/s)	(km/s)	(km/s)	(km/s)	(km/s)	(km/s)	(km/s)	(km/s)	(km/s)	(km/s)	(km/s)	(km/s)	(km/s)	(km/s)	(km/s)	(km/s)	(km/s)	(km/s)
10	2.17	0.21			2.21	0.12			2.23	0.11			2.40	0.21			2.47	0.21		
15	2.39	0.19			2.32	0.12			2.26	0.11			2.82	0.20			2.73	0.20		
20	2.63	0.18			2.51	0.10			2.46	0.09			3.04	0.19			2.88	0.18		
25	2.80	0.17	3.54	0.11	2.67	0.09	3.55	0.11	2.60	0.08	3.56	0.11	3.13	0.17	3.58	0.22	2.95	0.17	3.60	0.11
30	3.13	0.18	3.63	0.09	3.01	0.11	3.63	0.09	2.89	0.09	3.64	0.09	3.38	0.17	3.65	0.18	3.26	0.17	3.66	0.09
35	3.32	0.33	3.68	0.08	3.19	0.16	3.68	0.08	3.06	0.17	3.70	0.08	3.53	0.32	3.69	0.16	3.41	0.33	3.69	0.08
50			3.82	0.06			3.83	0.06			3.86	0.06			3.82	0.12			3.83	0.06
80			3.94	0.06			3.95	0.06			3.96	0.06			3.93	0.12			3.94	0.06
100			3.97	0.06			3.97	0.06			3.98	0.06			3.98	0.12			3.98	0.06
r.m.s.		0.13		0.055		0.07		0.055		0.07		0.055		0.13		0.09		0.13		0.055

segue Tab. 1

	Cell a3 (13.5; 41.5)				**Cell a4 (14.5; 41.5)**				**Cell a5 (15.5; 41.5)**				**Cell A1 (11.5; 40.5)**				**Cell A2 (12.5; 40.5)**			
Period	V_g	ρ_g	V_{ph}	ρ_{ph}	V_g	ρ_g	V_{ph}	ρ_{ph}	V_g	ρ_g	V_{ph}	ρ_{ph}	V_g	ρ_g	V_{ph}	ρ_{ph}	V_g	ρ_g	V_{ph}	ρ_{ph}
(s)	(km/s)	(km/s)	(km/s)	(km/s)	(km/s)	(km/s)	(km/s)	(km/s)	(km/s)	(km/s)	(km/s)	(km/s)	(km/s)	(km/s)	(km/s)	(km/s)	(km/s)	(km/s)	(km/s)	(km/s)
10	2.47	0.12			2.36	0.11			2.28	0.10			2.53	0.20			2.60	0.10		
15	2.56	0.14			2.38	0.09			2.31	0.08			3.07	0.16			2.99	0.08		
20	2.71	0.12			2.57	0.08			2.56	0.07			3.29	0.15			3.14	0.08		
25	2.75	0.12	3.61	0.11	2.63	0.08	3.59	0.11	2.66	0.08	3.58	0.11	3.31	0.15	3.63	0.11	3.17	0.08	3.64	0.11
30	3.07	0.12	3.67	0.09	2.94	0.10	3.66	0.09	2.93	0.09	3.66	0.09	3.45	0.16	3.67	0.09	3.36	0.08	3.67	0.09
35	3.23	0.18	3.71	0.08	3.09	0.17	3.71	0.08	3.03	0.16	3.72	0.08	3.59	0.32	3.71	0.08	3.51	0.16	3.70	0.08
50			3.84	0.06			3.87	0.06			3.88	0.06			3.82	0.06			3.81	0.06
80			3.95	0.06			3.96	0.06			3.95	0.06			3.92	0.06			3.93	0.06
100			3.98	0.06			3.98	0.06			3.98	0.06			3.98	0.06			3.98	0.06
r.m.s.		0.08		0.055		0.07		0.055		0.07		0.055		0.12		0.055		0.07		0.055
	Cell A3 (13.5; 40.5)				**Cell A4 (14.5; 40.5)**				**Cell A5 (15.5; 40.5)**				**Cell A6 (16.5; 40.5)**				**Cell B1 (11.5; 39.5)**			
Period	V_g	ρ_g	V_{ph}	ρ_{ph}	V_g	ρ_g	V_{ph}	ρ_{ph}	V_g	ρ_g	V_{ph}	ρ_{ph}	V_g	ρ_g	V_{ph}	ρ_{ph}	V_g	ρ_g	V_{ph}	ρ_{ph}
(s)	(km/s)	(km/s)	(km/s)	(km/s)	(km/s)	(km/s)	(km/s)	(km/s)	(km/s)	(km/s)	(km/s)	(km/s)	(km/s)	(km/s)	(km/s)	(km/s)	(km/s)	(km/s)	(km/s)	(km/s)
10	2.55	0.11			2.36	0.20			2.25	0.11			2.20	0.12			2.51	0.10		
15	2.74	0.12			2.45	0.17			2.33	0.08			2.31	0.09			2.95	0.10		
20	2.89	0.11			2.63	0.15			2.53	0.07			2.51	0.08			3.16	0.10		
25	2.96	0.10	3.65	0.11	2.76	0.15	3.64	0.11	2.70	0.08	3.62	0.22	2.77	0.09	3.61	0.11	3.28	0.08	3.68	0.11
30	3.22	0.10	3.69	0.09	3.06	0.16	3.69	0.09	2.99	0.08	3.68	0.18	3.04	0.09	3.68	0.09	3.40	0.09	3.71	0.09
35	3.37	0.17	3.72	0.08	3.20	0.32	3.73	0.08	3.13	0.17	3.73	0.16	3.21	0.17	3.73	0.08	3.52	0.16	3.74	0.08
50			3.83	0.06			3.85	0.06			3.86	0.12			3.87	0.06			3.83	0.06
80			3.94	0.06			3.94	0.06			3.94	0.12			3.93	0.06			3.92	0.06
100			3.98	0.06			3.98	0.06			3.98	0.12			3.98	0.06			3.99	0.06
r.m.s.		0.07		0.055		0.12		0.055		0.07		0.09		0.07		0.055		0.07		0.055

segue Tab. 1

	Cell B2 (12.5; 39.5)				**Cell B3 (13.5; 39.5)**				**Cell B4 (14.5; 39.5)**				**Cell B5 (15.5; 39.5)**				**Cell B6 (16.5; 39.5)**			
Period	V_g	ρ_g	V_{ph}	ρ_{ph}	V_g	ρ_g	V_{ph}	ρ_{ph}	V_g	ρ_g	V_{ph}	ρ_{ph}	V_g	ρ_g	V_{ph}	ρ_{ph}	V_g	ρ_g	V_{ph}	ρ_{ph}
(s)	(km/s)	(km/s)	(km/s)	(km/s)	(km/s)	(km/s)	(km/s)	(km/s)	(km/s)	(km/s)	(km/s)	(km/s)	(km/s)	(km/s)	(km/s)	(km/s)	(km/s)	(km/s)	(km/s)	(km/s)
10	2.53	0.10			2.47	0.11			2.34	0.11			2.19	0.10			2.11	0.10		
15	2.85	0.11			2.69	0.10			2.50	0.09			2.36	0.09			2.27	0.08		
20	3.02	0.10			2.85	0.09			2.68	0.08			2.56	0.08			2.47	0.07		
25	3.16	0.08	3.68	0.11	3.02	0.08	3.68	0.11	2.89	0.08	3.67	0.11	2.78	0.08	3.66	0.11	2.73	0.07	3.65	0.22
30	3.30	0.08	3.70	0.09	3.21	0.09	3.70	0.09	3.11	0.08	3.70	0.09	3.05	0.08	3.70	0.09	3.02	0.08	3.70	0.18
35	3.44	0.16	3.73	0.08	3.36	0.16	3.73	0.08	3.28	0.16	3.74	0.08	3.24	0.16	3.75	0.08	3.25	0.16	3.75	0.16
50			3.81	0.06			3.82	0.06			3.84	0.06			3.85	0.06			3.86	0.12
80			3.92	0.06			3.93	0.06			3.93	0.06			3.92	0.06			3.92	0.12
100			3.99	0.06			3.99	0.06			3.98	0.06			3.98	0.06			3.98	0.12
r.m.s.		0.07		0.055		0.07		0.055		0.07		0.055		0.07		0.055		0.07		0.09
	Cell C1 (11.5; 38.5)				**Cell C2 (12.5; 38.5)**				**Cell C3 (13.5; 38.5)**				**Cell C4 (14.5; 38.5)**				**Cell C5 (15.5; 38.5)**			
Period	V_g	ρ_g	V_{ph}	ρ_{ph}	V_g	ρ_g	V_{ph}	ρ_{ph}	V_g	ρ_g	V_{ph}	ρ_{ph}	V_g	ρ_g	V_{ph}	ρ_{ph}	V_g	ρ_g	V_{ph}	ρ_{ph}
(s)	(km/s)	(km/s)	(km/s)	(km/s)	(km/s)	(km/s)	(km/s)	(km/s)	(km/s)	(km/s)	(km/s)	(km/s)	(km/s)	(km/s)	(km/s)	(km/s)	(km/s)	(km/s)	(km/s)	(km/s)
10	2.44	0.20			2.41	0.20			2.34	0.11			2.25	0.11			2.16	0.10		
15	2.73	0.17			2.63	0.17			2.52	0.10			2.45	0.08			2.39	0.08		
20	2.91	0.15			2.80	0.15			2.71	0.08			2.66	0.07			2.62	0.07		
25	3.19	0.14	3.74	0.11	3.10	0.14	3.73	0.11	3.01	0.08	3.72	0.11	2.93	0.07	3.70	0.11	2.87	0.07	3.68	0.22
30	3.34	0.16	3.75	0.09	3.25	0.16	3.74	0.09	3.17	0.08	3.73	0.09	3.11	0.08	3.72	0.09	3.07	0.08	3.72	0.18
35	3.48	0.32	3.78	0.08	3.41	0.32	3.77	0.08	3.34	0.16	3.76	0.08	3.28	0.16	3.76	0.08	3.26	0.16	3.75	0.16
50			3.84	0.06			3.83	0.06			3.83	0.06			3.84	0.06			3.85	0.12
80			3.93	0.06			3.92	0.06			3.92	0.06			3.92	0.06			3.92	0.12
100			3.99	0.06			3.99	0.06			3.99	0.06			3.98	0.06			3.98	0.12
r.m.s.	0.12		0.055		0.12		0.055	0.12		0.07		0.055		0.07		0.055		0.07		0.09

segue Tab. 1

	Cell C6 (16.5; 38.5)				Cell D1 (11.5; 37.5)				Cell D2 (12.5; 37.5)			
Period	V_g	ρ_g	V_{ph}	ρ_{ph}	V_g	ρ_g	V_{ph}	ρ_{ph}	V_g	ρ_g	V_{ph}	ρ_{ph}
(s)	(km/s)	(km/s)	(km/s)	(km/s)	(km/s)	(km/s)	(km/s)	(km/s)	(km/s)	(km/s)	(km/s)	(km/s)
10	2.12	0.10			2.38	0.20			2.33	0.20		
15	2.32	0.08			2.61	0.16			2.54	0.16		
20	2.54	0.07			2.80	0.14			2.74	0.14		
25	2.80	0.07	3.67	0.22	3.18	0.14	3.77	0.11	3.13	0.14	3.76	0.11
30	3.03	0.08	3.71	0.18	3.32	0.16	3.78	0.09	3.27	0.16	3.77	0.09
35	3.25	0.16	3.76	0.16	3.50	0.32	3.81	0.08	3.46	0.32	3.80	0.08
50			3.85	0.12			3.86	0.06			3.86	0.06
80			3.92	0.12			3.93	0.06			3.92	0.06
100			3.98	0.12			3.99	0.06			3.99	0.06
r.m.s.		0.07		0.09		0.12		0.055		0.12		0.55
	Cell D3 (13.5; 37.5)				Cell D4 (14.5; 37.5)				Cell D5 (15.5; 37.5)			
Period	V_g	ρ_g	V_{ph}	ρ_{ph}	V_g	ρ_g	V_{ph}	ρ_{ph}	V_g	ρ_g	V_{ph}	ρ_{ph}
(s)	(km/s)	(km/s)	(km/s)	(km/s)	(km/s)	(km/s)	(km/s)	(km/s)	(km/s)	(km/s)	(km/s)	(km/s)
10	2.27	0.20			2.22	0.20			2.18	0.20		
15	2.47	0.16			2.44	0.16			2.45	0.16		
20	2.70	0.14			2.70	0.15			2.71	0.14		
25	3.07	0.15	3.74	0.22	3.03	0.16	3.71	0.22	2.99	0.15	3.70	0.22
30	3.23	0.16	3.75	0.18	3.19	0.17	3.74	0.18	3.16	0.16	3.72	0.18
35	3.40	0.32	3.78	0.16	3.34	0.32	3.77	0.16	3.31	0.32	3.77	0.16
50			3.85	0.12			3.85	0.12			3.85	0.12
80			3.92	0.12			3.92	0.12			3.92	0.12
100			3.98	0.12			3.98	0.12			3.98	0.12
r.m.s.		0.12		0.09		0.12		0.09		0.12		0.09

defined by V_p, V_s, density and thickness (h). Each parameter of the structure can be independent (the parameter is variable and can be well resolved by the data), dependent (the parameter has a fixed relationship with an independent parameter) or fixed (the parameter is held constant during the inversion, accordingly with independent geophysical evidences). For the cells with a low path-coverage, both in phase and group velocity, we have adopted a parametrization with a number of independent parameters lower than elsewhere. The adopted parameterization for each cell is given in table 2.

3. - AVERAGE CELLULAR LITHOSPHERIC MODELS FROM GEOPHYSICAL DATA

The available interpretations of the seismic profiles that cross most of the peninsula and adjacent seas together with other information available from literature (Bally *et alii,* 1986; Calcagnile *et alii*, 1982; Catalano *et alii*, 1996 and 2001; Cernobori *et alii*, 1996; Chimera *et alii*, 2003; Cristofolini *et alii*, 1985; De Gori *et alii*, 2001; Della Vedova *et alii,* 1989 and 1991; De Matteis *et alii*, 2000; De Voggd *et alii*, 1992; Doglioni *et alii*, 2001; Ferrucci *et alii*, 1991; Finetti, 1982; Finetti & Del Ben, 1986; Finetti *et alii*, 2001; Improta *et alii*, 2000; Kern & Schenk, 1988; Mantovani *et alii*, 1985; Marson *et alii*, 1995; Morelli, 1998; Monstaanpour, 1984; Pepe *et alii*, 2000; Pialli *et alii*, 1995; Scarascia & Cassinis, 1992; Scarascia *et alii*, 1994; Venisti *et alii*, 2003) are used to fix h and V_P of the uppermost crustal layers, assuming that they are formed by Poissonian solids. In table 2 the fixed V_p, V_s and h of the upper crustal layers are reported for each cell. The thickness of the water layer is chosen accordingly with standard bathymetric maps. The density of all the layers is in agreement with the Nafe-Drake relation, as reported by Ludwig *et alii* (1970): one and the same relation between V_p, V_s and density has been used for all the dependent parameters in the inversion, in most of the cells of the study area. The deviations from this rule can be seen in table 2. The structure below the

Tab. 2 - *Parametrization used in the non-linear inversion. Grey area: h (thickness), V_s and V_p of each layer. The uppermost layers are fixed on the base of available literature* (BALLY *et alii*, 1986; CALCAGNILE *et alii*, 1982; CATALANO *et alii*, 1996 and 2001; CERNOBORI *et alii*, 1996; CHIMERA *et alii*, 2003; CRISTOFOLINI *et alii*, 1985; DE GORI *et alii*, 2001; DELLA VEDOVA *et alii,* 1989 and 1991; DE MATTEIS *et alii*, 2000; DE VOGGD *et alii*, 1992; DOGLIONI *et alii*, 2001; FERRUCCI *et alii*, 1991; FINETTI, 1982; FINETTI & DEL BEN, 1986; FINETTI *et alii*, 2001; IMPROTA *et alii*, 2000; KERN & SCHENK, 1988; MANTOVANI *et alii*, 1985; MARSON *et alii*, 1995; MORELLI, 1998; MONSTAANPOUR, 1984; PEPE *et alii*, 2000; PIALLI *et alii*, 1995; SCARASCIA & CASSINIS, 1992; SCARASCIA *et alii*, 1994; VENISTI *et alii*, 2003). *The variable parameters are Pi, with i= 1, … 5 for thickness and i= 6, … 10 for V_s when the parameters are 10, and Pi, with i= 1, … 4 for thickness and i= 5, … 8 for V_s when the parameters are 8. White area: step (δPi) and variability range for each parameter Pi. The inverted velocities have always the second decimal value equal to 0 or 5. This rule is not in the fixed upper crust. The range of variability of the parameters h and V_s for each layer of the chosen solutions are deducible from this table.*

Cell c0 (10.5; 43.5)			**Cell c1 (11.5; 43.5)**			**Cell c2 (12.5; 43.5)**			**Cell c3 (13.5; 43.5)**			**Cell b0 (10.5; 42.5)**			**Cell b1 (11.5; 42.5)**		
h	V_S	V_P	h	V_S	V_P	h	V_S	V_P	h	V_S	V_P	h	V_S	V_P	h	V_S	V_P
(km)	(km/s)	(km/s)	(km)	(km/s)	(km/s)	(km)	(km/s)	(km/s)	(km)	(km/s)	(km/s)	(km)	(km/s)	(km/s)	(km)	(km/s)	(km/s)
4	2.20	3.80	4	2.20	3.80	0.5	1.60	2.65	1.1	1.55	2.65	0.5	0.00	1.52	0.25	3.00	5.50
1	2.65	4.60	1	2.65	4.60	1	2.30	3.60	2.4	2.08	3.60	0.5	3.00	5.50	0.75	3.50	6.10
3	3.00	5.20	3	3.00	5.20	1	3.00	5.50	1.5	3.18	5.50	6	2.65	5.00	6	2.65	5.00
P1	P6	P6x1.73	P1	P6	P6x1.73	1.5	3.50	6.10	1	3.50	6.10	P1	P6	P6x1.73	P1	P6	P6x1.73
P2	P7	P7x1.73	P2	P7	P7x1.73	P1	P6	P6x1.73	P1	P6	P6x1.73	P2	P7	P7x1.73	P2	P7	P7x1.73
P3	P8	P8x1.73	P3	P8	P8x1.73	P2	P7	P7x1.73	P2	P7	P7x1.73	P3	P8	P8x1.73	P3	P8	P8x1.73
P4	P9	P9x1.73	P4	P9	P9x1.73	P3	P8	P8x1.73	P3	P8	P8x1.73	P4	P9	P9x1.73	P4	P9	P9x1.73
P5	P10	P10x1.73	P5	P10	P10x1.73	P4	P9	P9x1.73	P4	P9	P9x1.73	P5	P10	P10x1.73	P5	P10	P10x1.73
						P5	P10	P10x1.73	P5	P10	P10x1.73						
h	Step	Range	h	Step	Range	h	Step	Range	h	Step	Range	h	Step	Range	h	Step	Range
(km)	(km)	(km)	(km)	(km)	(km)	(km)	(km)	(km)	(km)	(km)	(km)	(km)	(km)	(km)	(km)	(km)	(km)
P1	4	4-16	P1	8	6-14	P1	5	4-19	P1	4	5.5-17.5	P1	10	10-20	P1	5	5-20
P2	20	20-40	P2	10	10-30	P2	5	5-25	P2	6	5-29	P2	20	15-35	P2	30	15-45
P3	20	15-35	P3	10	15-35	P3	10	25-45	P3	5	10-50	P3	30	20-50	P3	20	20-60
P4	60	60-120	P4	65	50-135	P4	25	60-110	P4	10	20-110	P4	50	60-110	P4	60	30-90
P5	60	60-120	P5	60	60-120	P5	60	60-120	P5	30	40-130	P5	55	70-125	P5	50	70-120
V_S	Step	Range	V_S	Step	Range	V_S	Step	Range	V_S	Step	Range	V_S	Step	Range	V_S	Step	Range
(km/s)	(km/s)	(km/s)	(km/s)	(km/s)	(km/s)	(km/s)	(km/s)	(km/s)	(km/s)	(km/s)	(km/s)	(km/s)	(km/s)	(km/s)	(km/s)	(km/s)	(km/s)
P6	0.20	2.70-3.90	P6	0.10	2.30-3.80	P6	0.10	2.10-3.40	P6	0.05	2.35-4.25	P6	0.30	2.20-4.30	P6	0.30	2.20-3.10
P7	0.20	3.50-4.50	P7	0.20	3.50-4.40	P7	0.20	2.35-4.55	P7	0.10	3.30-4.50	P7	0.40	3.35-4.55	P7	0.40	2.80-4.40
P8	0.25	3.75-4.75	P8	0.30	3.55-4.45	P8	0.15	3.40-4.60	P8	0.20	3.35-4.75	P8	0.30	3.6-4.8	P8	0.40	3.65-4.45
P9	0.40	4.00-4.80	P9	0.20	4.00-4.80	P9	0.20	4.00-4.80	P9	0.10	4.00-4.80	P9	0.25	4.00-4.75	P9	0.20	4.00-4.80
P10	0.40	4.00-4.80	P10	0.40	4.00-4.80	P10	0.30	4.00-4.90	P10	0.20	4.00-4.80	P10	0.30	4.00-4.90	P10	0.25	4.00-4.75

segue Tab. 2

Cell b2 (12.5; 42.5)			**Cell b3 (13.5; 42.5)**			**Cell a1 (11.5; 41.5)**			**Cell a2 (12.5; 41.5)**			**Cell a3 (13.5; 41.5)**			**Cell a4 (14.5; 41.5)**		
h	V_S	V_P	h	V_S	V_P	h	V_S	V_P	h	V_S	V_P	h	V_S	V_P	h	V_S	V_P
(km)	(km/s)	(km/s)	(km)	(km/s)	(km/s)	(km)	(km/s)	(km/s)	(km)	(km/s)	(km/s)	(km)	(km/s)	(km/s)	(km)	(km/s)	(km/s)
1.2	1.60	2.65	1.2	1.55	2.65	1	0.00	1.52	1	0.00	1.52	3	1.87	3.25	2.6	2.13	3.70
0.8	2.30	3.60	0.8	2.13	3.70	2.7	1.33	2.30	2.7	1.32	2.30	2	2.19	3.80	2.5	2.45	4.25
1.5	3.00	5.50	1.5	3.10	5.35	1	2.90	5.00	1	3.06	5.30	3	3.26	5.65	2.9	3.06	5.30
1	3.50	6.10	1	3.61	6.25	2	3.30	5.70	2	3.25	5.60	2	3.45	6.00	3	4.15	5.50
P1	P6	P6x1.73	P1	P6	P6x1.73	P1	P5	P6x1.73	P1	P6	P6x1.73	P1	P6	P6x1.73	P1	P6	P6x1.73
P2	P7	P7x1.73	P2	P7	P7x1.73	P2	P6	P7x1.73	P2	P7	P7x1.73	P2	P7	P7x1.73	P2	P7	P7x1.73
P3	P8	P8x1.73	P3	P8	P8x1.73	P3	P7	P8x1.73	P3	P8	P8x1.73	P3	P8	P8x1.73	P3	P8	P8x1.73
P4	P9	P9x1.73	P4	P9	P9x1.73	P4	P8	P9x1.73	P4	P9	P9x1.73	P4	P9	P9x1.73	P4	P9	P9x1.73
P5	P10	P10x1.73	P5	P10	P10x1.73				P5	P10	P10x1.73	P5	P10	P10x1.73	P5	P10	P10x1.73
h	Step	Range	h	Step	Range	h	Step	Range	h	Step	Range	h	Step	Range	h	Step	Range
(km)	(km)	(km)	(km)	(km)	(km)	(km)	(km)	(km)	(km)	(km)	(km)	(km)	(km)	(km)	(km)	(km)	(km)
P1	6	9-21	P1	4	3-19	P1	20	20-40	P1	10	15-35	P1	5	11-26	P1	6	5.5-23.5
P2	10	15-25	P2	5	8-28	P2	20	5-45	P2	10	15-25	P2	4	10-18	P2	6	5-35
P3	15	15-30	P3	15	15-45	P3	50	50-100	P3	30	15-45	P3	20	15-35	P3	10	6-56
P4	50	50-100	P4	30	65-125	P4	60	60-120	P4	60	40-100	P4	60	60-120	P4	15	40-100
P5	60	40-160	P5	40	40-120				P5	70	60-130	P5	30	70-130	P5	30	30-120
V_S	Step	Range	V_S	Step	Range	V_S	Step	Range	V_S	Step	Range	V_S	Step	Range	V_S	Step	Range
(km/s)	(km/s)	(km/s)	(km/s)	(km/s)	(km/s)	(km/s)	(km/s)	(km/s)	(km/s)	(km/s)	(km/s)	(km/s)	(km/s)	(km/s)	(km/s)	(km/s)	(km/s)
P6	0.15	2.35-3.85	P6	0.10	2.20-4.10	P5	0.20	3.50-4.10	P6	0.30	3.05-4.25	P6	0.20	2.95-4.15	P6	0.05	2.40-4.40
P7	0.25	2.40-4.40	P7	0.10	3.20-4.40	P6	0.45	3.70-4.60	P7	0.30	3.50-4.40	P7	0.30	3.35-4.55	P7	0.10	3.25-4.75
P8	0.30	3.55-4.75	P8	0.15	3.60-4.65	P7	0.80	4.00-4.80	P8	0.80	3.85-4.65	P8	0.15	3.60-4.65	P8	0.10	3.40-4.70
P9	0.30	4.05-4.95	P9	0.10	4.00-4.80	P8	0.80	4.00-4.80	P9	0.40	4.00-4.80	P9	0.20	4.00-4.80	P9	0.05	4.00-4.80
P10	0.20	4.00-4.80	P10	0.20	4.00-4.80				P10	0.40	4.00-4.80	P10	0.40	4.00-4.80	P10	0.10	4.00-4.80

segue Tab. 2

Cell A6 (16.5; 40.5)			**Cell B1 (11.5; 39.5)**			**Cell B2 (12.5; 39.5)**			**Cell B3 (13.5; 39.5)**			**Cell B4 (14.5; 39.5)**			**Cell B5 (15.5; 39.5)**		
h	V_S	V_P	h	V_S	V_P	h	V_S	V_P	h	V_S	V_P	h	V_S	V_P	h	V_S	V_P
(km)	(km/s)	(km/s)	(km)	(km/s)	(km/s)	(km)	(km/s)	(km/s)	(km)	(km/s)	(km/s)	(km)	(km/s)	(km/s)	(km)	(km/s)	(km/s)
1.1	1.50	2.65	3	0.0	1.52	3	0.0	1.52	3.2	0.0	1.52	2.5	0.0	1.52	0.9	0.0	1.52
2.4	2.10	3.60	0.7	1.2	2.05	0.7	1.2	2.05	0.5	1.2	2.05	0.5	1.3	2.24	1.9	1.15	1.98
1.5	2.90	5.00	1	3.45	6.0	1	3.45	6.0	1	3.45	6.0	2	3.45	6.0	3	2.9	5.0
4	3.49	6.05	2	4.0	6.9	2	4.0	6.9	2	4.0	6.9	1.5	4.0	6.9			
P1	P6	P6x1.73	P1	P6	P6x1.73	P1	P6	P6x1.73	P1	P6	P6x1.73	P1	P6	P6x1.73	P1	P6	P6x1.73
P2	P7	P7x1.73	P2	P7	P7x2.00	P2	P7	P7x2.00	P2	P7	P7x2.00	P2	P7	P7x2.00	P2	P7	P7x1.73
P3	P8	P8x1.73	P3	P8	P8x2.00	P3	P8	P8x2.00	P3	P8	P8x2.00	P3	P8	P8x2.00	P3	P8	P8x1.73
P4	P9	P9x1.73	P4	P9	P9x2.00	P4	P9	P9x2.00	P4	P9	P9x2.00	P4	P9	P9x2.00	P4	P9	P9x1.73
P5	P10	P10x1.73	P5	P10	P10x2.00	P5	P10	P10x2.00	P5	P10	P10x2.00	P5	P10	P10x2.00	P5	P10	P10x1.73
h	Step	Range	h	Step	Range	h	Step	Range	h	Step	Range	h	Step	Range	h	Step	Range
(km)	(km)	(km)	(km)	(km)	(km)	(km)	(km)	(km)	(km)	(km)	(km)	(km)	(km)	(km)	(km)	(km)	(km)
P1	2.5	4.5-12	P1	4.5	6.5-20	P1	4	2-18	P1	3	3.5-12.5	P1	4	5-21	P1	2	5-29
P2	10	10-40	P2	10	11-31	P2	7	8-29	P2	4	6-18	P2	10	10-30	P2	10	5-25
P3	30	15-45	P3	40	11-51	P3	20	20-60	P3	20	30-70	P3	40	25-65	P3	20	20-60
P4	70	50-120	P4	60	45-105	P4	50	45-95	P4	70	35-105	P4	30	35-95	P4	20	15-95
P5	60	60-120	P5	70	60-130	P5	80	55-135	P5	70	60-130	P5	55	15-130	P5	45	35-125
V_S	Step	Range	V_S	Step	Range	V_S	Step	Range	V_S	Step	Range	V_S	Step	Range	V_S	Step	Range
(km/s)	(km/s)	(km/s)	(km/s)	(km/s)	(km/s)	(km/s)	(km/s)	(km/s)	(km/s)	(km/s)	(km/s)	(km/s)	(km/s)	(km/s)	(km/s)	(km/s)	(km/s)
P6	0.20	2.40-4.40	P6	0.3	3.1-4.6	P6	0.2	3.1-4.5	P6	0.15	3.60-4.65	P6	0.1	2.4-4.6	P6	0.05	2.5-4.6
P7	0.30	3.40-4.60	P7	0.3	2.8-4.6	P7	0.25	2.80-4.55	P7	0.2	2.5-4.1	P7	0.3	3.25-4.75	P7	0.2	3.2-4.6
P8	0.35	3.45-4.85	P8	0.25	3.40-4.65	P8	0.4	3.3-4.5	P8	0.1	3.7-4.7	P8	0.1	3.5-4.7	P8	0.1	3.45-4.85
P9	0.30	4.00-4.90	P9	0.35	4.0-4.7	P9	0.3	4.0-4.9	P9	0.25	4.00-4.75	P9	0.4	4.0-4.8	P9	0.1	4.0-4.8
P10	0.40	4.00-4.80	P10	0.3	4.0-4.9	P10	0.3	4.0-4.9	P10	0.3	4.0-4.9	P10	0.3	4.0-4.9	P10	0.1	4.0-4.8

segue Tab. 2

Cell A6 (16.5; 40.5)			**Cell B1 (11.5; 39.5)**			**Cell B2 (12.5; 39.5)**			**Cell B3 (13.5; 39.5)**			**Cell B4 (14.5; 39.5)**			**Cell B5 (15.5; 39.5)**		
h	V_S	V_P	h	V_S	V_P	h	V_S	V_P	h	V_S	V_P	h	V_S	V_P	h	V_S	V_P
(km)	(km/s)	(km/s)	(km)	(km/s)	(km/s)	(km)	(km/s)	(km/s)	(km)	(km/s)	(km/s)	(km)	(km/s)	(km/s)	(km)	(km/s)	(km/s)
1.1	1.50	2.65	3	0.0	1.52	3	0.0	1.52	3.2	0.0	1.52	2.5	0.0	1.52	0.9	0.0	1.52
2.4	2.10	3.60	0.7	1.2	2.05	0.7	1.2	2.05	0.5	1.2	2.05	0.5	1.3	2.24	1.9	1.15	1.98
1.5	2.90	5.00	1	3.45	6.0	1	3.45	6.0	1	3.45	6.0	2	3.45	6.0	3	2.9	5.0
4	3.49	6.05	2	4.0	6.9	2	4.0	6.9	2	4.0	6.9	1.5	4.0	6.9			
P1	P6	P6x1.73	P1	P6	P6x1.73	P1	P6	P6x1.73	P1	P6	P6x1.73	P1	P6	P6x1.73	P1	P6	P6x1.73
P2	P7	P7x1.73	P2	P7	P7x2.00	P2	P7	P7x2.00	P2	P7	P7x2.00	P2	P7	P7x2.00	P2	P7	P7x1.73
P3	P8	P8x1.73	P3	P8	P8x2.00	P3	P8	P8x2.00	P3	P8	P8x2.00	P3	P8	P8x2.00	P3	P8	P8x1.73
P4	P9	P9x1.73	P4	P9	P9x2.00	P4	P9	P9x2.00	P4	P9	P9x2.00	P4	P9	P9x2.00	P4	P9	P9x1.73
P5	P10	P10x1.73	P5	P10	P10x2.00	P5	P10	P10x2.00	P5	P10	P10x2.00	P5	P10	P10x2.00	P5	P10	P10x1.73
h	Step	Range	h	Step	Range	h	Step	Range	h	Step	Range	h	Step	Range	h	Step	Range
(km)	(km)	(km)	(km)	(km)	(km)	(km)	(km)	(km)	(km)	(km)	(km)	(km)	(km)	(km)	(km)	(km)	(km)
P1	2.5	4.5-12	P1	4.5	6.5-20	P1	4	2-18	P1	3	3.5-12.5	P1	4	5-21	P1	2	5-29
P2	10	10-40	P2	10	11-31	P2	7	8-29	P2	4	6-18	P2	10	10-30	P2	10	5-25
P3	30	15-45	P3	40	11-51	P3	20	20-60	P3	20	30-70	P3	40	25-65	P3	20	20-60
P4	70	50-120	P4	60	45-105	P4	50	45-95	P4	70	35-105	P4	30	35-95	P4	20	15-95
P5	60	60-120	P5	70	60-130	P5	80	55-135	P5	70	60-130	P5	55	15-130	P5	45	35-125
V_S	Step	Range	V_S	Step	Range	V_S	Step	Range	V_S	Step	Range	V_S	Step	Range	V_S	Step	Range
(km/s)	(km/s)	(km/s)	(km/s)	(km/s)	(km/s)	(km/s)	(km/s)	(km/s)	(km/s)	(km/s)	(km/s)	(km/s)	(km/s)	(km/s)	(km/s)	(km/s)	(km/s)
P6	0.20	2.40-4.40	P6	0.3	3.1-4.6	P6	0.2	3.1-4.5	P6	0.15	3.60-4.65	P6	0.1	2.4-4.6	P6	0.05	2.5-4.6
P7	0.30	3.40-4.60	P7	0.3	2.8-4.6	P7	0.25	2.80-4.55	P7	0.2	2.5-4.1	P7	0.3	3.25-4.75	P7	0.2	3.2-4.6
P8	0.35	3.45-4.85	P8	0.25	3.40-4.65	P8	0.4	3.3-4.5	P8	0.1	3.7-4.7	P8	0.1	3.5-4.7	P8	0.1	3.45-4.85
P9	0.30	4.00-4.90	P9	0.35	4.0-4.7	P9	0.3	4.0-4.9	P9	0.25	4.00-4.75	P9	0.4	4.0-4.8	P9	0.1	4.0-4.8
P10	0.40	4.00-4.80	P10	0.3	4.0-4.9	P10	0.3	4.0-4.9	P10	0.3	4.0-4.9	P10	0.3	4.0-4.9	P10	0.1	4.0-4.8

segue Tab. 2

Cell B6 (16.5; 39.5)			**Cell C1 (11.5; 38.5)**			**Cell C2 (12.5; 38.5)**			**Cell C3 (13.5; 38.5)**			**Cell C4 (14.5; 38.5)**			**Cell C5 (15.5; 38.5)**		
h	V_S	V_P	h	V_S	V_P	h	V_S	V_P	h	V_S	V_P	h	V_S	V_P	h	V_S	V_P
(km)	(km/s)	(km/s)	(km)	(km/s)	(km/s)	(km)	(km/s)	(km/s)	(km)	(km/s)	(km/s)	(km)	(km/s)	(km/s)	(km)	(km/s)	(km/s)
4	2.45	4.25	1.5	0.0	1.52	1	0.0	1.52	2	0.0	1.52	2.2	0.0	1.52	1	0.0	1.52
9	2.8	4.85	0.9	1.1	1.9	1.4	1.1	1.9	0.4	1.1	1.9	0.2	1.0	1.75	2	2.6	4.5
			0.4	2.31	4.0	0.4	2.31	4.0	0.4	2.31	4.0	0.4	2.31	4.0			
			4.2	2.90	5.0	3.2	2.9	5.0	3.2	2.9	5.0	3.2	3.55	6.15			
P1	P6	P6x1.73	P1	P6	P6x1.73	P1	P6	P6x1.73	P1	P6	P6x1.73	P1	P6	P6x1.73	P1	P6	P6x1.73
P2	P7	P7x1.73	P2	P7	P7x1.73	P2	P7	P7x1.73	P2	P7	P7x1.73	P2	P7	P7x1.73	P2	P7	P7x1.73
P3	P8	P8x1.73	P3	P8	P8x1.73	P3	P8	P8x1.73	P3	P8	P8x1.73	P3	P8	P8x1.73	P3	P8	P8x1.73
P4	P9	P9x1.73	P4	P9	P9x1.73	P4	P9	P9x1.73	P4	P9	P9x1.73	P4	P9	P9x1.73	P4	P9	P9x1.73
P5	P10	P10x1.73	P5	P10	P10x1.73	P5	P10	P10x1.73	P5	P10	P10x1.73	P5	P10	P10x1.73	P5	P10	P10x1.73
h	Step	Range	h	Step	Range	h	Step	Range	h	Step	Range	h	Step	Range	h	Step	Range
(km)	(km)	(km)	(km)	(km)	(km)	(km)	(km)	(km)	(km)	(km)	(km)	(km)	(km)	(km)	(km)	(km)	(km)
P1	8	12-20	P1	9	12-30	P1	10	14-34	P1	2	7-25	P1	2	5-19	P1	4	2-22
P2	12	12-36	P2	30	15-45	P2	30	20-50	P2	5	5-30	P2	4	10-34	P2	4	4-28
P3	20	25-45	P3	30	40-70	P3	25	25-75	P3	20	20-80	P3	5	20-50	P3	10	5-35
P4	50	45-95	P4	40	40-80	P4	40	45-85	P4	30	25-85	P4	15	25-100	P4	50	60-110
P5	60	65-125	P5	55	45-100	P5	40	50-90	P5	60	55-115	P5	35	20-125	P5	60	70-130
V_S	Step	Range	V_S	Step	Range	V_S	Step	Range	V_S	Step	Range	V_S	Step	Range	V_S	Step	Range
(km/s)	(km/s)	(km/s)	(km/s)	(km/s)	(km/s)	(km/s)	(km/s)	(km/s)	(km/s)	(km/s)	(km/s)	(km/s)	(km/s)	(km/s)	(km/s)	(km/s)	(km/s)
P6	0.4	2.8-4.4	P6	0.4	3.35-4.55	P6	0.3	3.15-4.65	P6	0.1	2.55-4.35	P6	0.05	2.45-4.55	P6	0.15	2.30-4.25
P7	0.8	2.9-4.5	P7	0.5	3.2-4.7	P7	0.25	3.25-4.5	P7	0.05	3.05-4.55	P7	0.2	3.05-4.55	P7	0.4	3.15-4.75
P8	0.4	3.5-4.7	P8	0.3	3.7-4.6	P8	0.6	3.4-4.6	P8	0.1	3.6-4.8	P8	0.1	3.3-4.7	P8	0.2	3.1-4.7
P9	0.4	4.0-4.8	P9	0.2	4.0-4.8	P9	0.2	4.0-4.8	P9	0.2	4.0-4.8	P9	0.05	4.0-4.8	P9	0.2	4.0-4.8
P10	0.8	4.0-4.8	P10	0.4	4.0-4.8	P10	0.4	4.0-4.8	P10	0.4	4.0-4.8	P10	0.1	4.0-4.8	P10	0.25	4.00-4.75

segue Tab. 2

Cell C6 (16.5; 38.5)			**Cell D1 (11.5; 37.5)**			**Cell D2 (12.5; 37.5)**			**Cell D3 (13.5; 37.5)**			**Cell D4 (14.5; 37.5)**			**Cell D5 (15.5; 37.5)**		
h	V_S	V_P	h	V_S	V_P	h	V_S	V_P	h	V_S	V_P	h	V_S	V_P	h	V_S	V_P
(km)	(km/s)	(km/s)	(km)	(km/s)	(km/s)	(km)	(km/s)	(km/s)	(km)	(km/s)	(km/s)	(km)	(km/s)	(km/s)	(km)	(km/s)	(km/s)
4	2.5	4.3	0.5	0.00	1.52	0.25	0.00	1.52	2.5	1.73	3.00	3	1.73	3.00	2.5	0.0	1.52
9	2.85	4.9	2.5	1.73	3.00	2.75	1.85	3.20	2.5	2.60	4.50	2	2.60	4.50	1.6	2.25	3.9
			2	2.90	5.00	2	2.65	4.60	5	2.90	5.00	5	2.90	5.00	1.1	2.35	4.05
			5	3.45	6.00	5	2.95	5.10	P1	P5	P6x1.73	P1	P5	P6x1.73	2.8	3.35	5.8
P1	P6	P6x1.73	P1	P6	P6x1.73	P1	P6	P6x1.73	P2	P6	P7x1.73	P2	P6	P7x1.73	P1	P6	P6x1.73
P2	P7	P7x1.73	P2	P7	P7x1.73	P2	P7	P7x1.73	P3	P7	P8x1.73	P3	P7	P8x1.73	P2	P7	P7x1.73
P3	P8	P8x1.73	P3	P8	P8x1.73	P3	P8	P8x1.73	P4	P8	P9x1.73	P4	P8	P9x1.73	P3	P8	P8x1.73
P4	P9	P9x1.73	P4	P9	P9x1.73	P4	P9	P9x1.73							P4	P9	P9x1.73
P5	P10	P10x1.73	P5	P10	P10x1.73	P5	P10	P10x1.73							P5	P10	P10x1.73
h	Step	Range	h	Step	Range	h	Step	Range	h	Step	Range	h	Step	Range	h	Step	Range
(km)	(km)	(km)	(km)	(km)	(km)	(km)	(km)	(km)	(km)	(km)	(km)	(km)	(km)	(km)	(km)	(km)	(km)
P1	4	4-16	P1	20	15-35	P1	10	5-25	P1	5	15-35	P1	10	5-35	P1	10	15-25
P2	15	2.5-32.5	P2	15	10-25	P2	10	15-35	P2	30	25-55	P2	30	25-55	P2	15	20-35
P3	10	10-30	P3	40	15-55	P3	30	25-55	P3	40	60-100	P3	80	40-120	P3	25	20-45
P4	60	65-125	P4	50	50-100	P4	50	50-100	P4	80	60-140	P4	60	60-120	P4	40	70-110
P5	70	60-130	P5	60	60-120	P5	40	80-120							P5	60	65-125
V_S	Step	Range	V_S	Step	Range	V_S	Step	Range	V_S	Step	Range	V_S	Step	Range	V_S	Step	Range
(km/s)	(km/s)	(km/s)	(km/s)	(km/s)	(km/s)	(km/s)	(km/s)	(km/s)	(km/s)	(km/s)	(km/s)	(km/s)	(km/s)	(km/s)	(km/s)	(km/s)	(km/s)
P6	0.3	2.7-4.5	P6	0.20	3.15-4.35	P6	0.20	3.05-4.25	P5	0.10	3.20-4.40	P5	0.20	3.20-4.40	P6	0.25	3.0-4.5
P7	0.5	3.4-4.4	P7	0.40	3.50-4.30	P7	0.20	3.20-4.40	P6	0.30	3.45-4.65	P6	0.10	3.85-4.65	P7	0.4	3.3-4.5
P8	0.5	3.1-4.6	P8	0.20	3.85-4.65	P8	0.30	3.75-4.65	P7	0.40	4.00-4.80	P7	0.40	4.00-4.80	P8	0.35	3.45-4.85
P9	0.2	4.0-4.8	P9	0.40	4.00-4.80	P9	0.40	4.00-4.80	P8	0.80	4.00-4.80	P8	0.80	4.00-4.80	P9	0.4	4.0-4.8
P10	0.25	4.00-4.75	P10	0.40	4.00-4.80	P10	0.40	4.00-4.80							P10	0.8	4.0-4.8

inverted layers is the same for all the considered cells and it has been fixed accordingly with already published data (DU *et alii*, 1998).

In figure 2 (a & b) we plot all the solutions of the inversion, that is V_s versus depth, from the surface to 250 km, and the explored parameter's space (shadowed area).

For each cell we indicate the depth of the Mohorovicic discontinuity (M) and the solution that we select (bold line) following, as in PANZA *et alii* (2003), the criterion that a simple solution is preferable to one that is unnecessarily complicated (DEGROOT-HEDLIN & CONSTABLE, 1990). The structural models chosen for all the cells, whose uncertainty can be inferred from direct inspection of figure 2, satisfy (within the r.m.s. value used in our inversions, see tab. 1) the additional condition to be consistent, at periods greater than 35 s, with the group velocity values given by PASYANOS *et alii* (2001).

3.1. - THE CRUST

Cells c0-c3 and b0-b3 (see fig. 2a) are characterized by the presence of a relatively high velocity layer (V_s 3.0 km/s) in the uppermost crust, followed by one at low velocity (2.60 V_s 2.95 km/s) and less than about 10 km thick. In these cells the model in the uppermost 10 km is fixed according to the results obtained by CHIMERA *et alii* (2003), which use CROP-03 profile to define the sequence of the stratigraphic units, their density and V_p. The structures of cells b0-b3 and c3 are obtained considering the phase velocity data ranging from 25 s to 100 s and not from 30 s to 100 s as in CHIMERA *et alii* (2003) for the same area. The differences between our structures and those of CHIMERA *et alii* (2003) are negligible, and the use of a larger period range of the phase velocity dispersion confirms the findings of CHIMERA *et alii* (2003). In this Apenninic area, the lower crust above the Moho has the V_s in the range 3.1-4.0 km/s. More to the South, in cells a1-a5 (fig. 2a), a positive velocity gradient is present in the crust, reaching the velocity of about 3.75-3.95 km/s in the lower crust.

In cells A1-A3 (fig. 2a) and B1-B4 (fig. 2b) the sedimentary layer is very thin and it is followed by a layering consistent with standard schematic oceanic crustal models (e.g. PANZA, 1984). In A5-A6 a low velocity layer appears in the upper crust and it is just above the Moho in A4, C4 and D5 with the V_s in the range 2.75-3.25 km/s. All the other cells are characterized by a thick crust, where the velocity of the sediments increases with increasing depth. With the exception of cells b2, C3-C5 and D5, all the cells in the continental region and in the Tyrrhenian offshore of Sicily, are characterized by a layer, just above the Moho, with V_s in the range 3.5-4.0 km/s. The location of the Moho depth in each cell is defined within a few kilometres.

3..2. - THE MOHO AND THE UPPERMOST UPPER MANTLE.

In the Northern Apenninic area (cells from c0 to c3 and from b1 to b3) and in cell b0, which contains Elba island, the Moho depth falls in the range 28-39 km with the maximum value in c1 and the minimum value in cells b0-b2 (fig. 2a). In the structures of c0-c3, b0 and b3 cells, the lid just below the Moho is characterized by relatively high V_s, in the range 4.35-4.60 km/s. The velocity of the lid increases with the depth in cells c2-c3 and b3, reaching values between 4.6 km/s and 4.8 km/s. In cells c1-c3 and b3 the asthenosphere starts below this high velocity layer at the depth of about 130-175 km. In cell c0, instead, the lid has a thickness of about 35 km. In cells b1 and b2, below the Moho, a relatively low velocity layer ($4.05 \leq V_s \leq 4.15$ km/s) and 15-20 km thick is present. This layer defined mantle wedge (layer with V_s less than about 4.2 km/sec in the uppermost mantle that overlies a high velocity lid with V_s greater than about 4.5 km/sec) by PANZA *et alii* (2003), with a percentage of partial melting of about 1-2% accordingly with BOTTINGA & STEINMETZ, 1979) could be associated to the presence of the inactive recent volcanoes of Amiata, Vulsini in b1 and Cimino, Vico, Sabatini in b2. The structural model of cell b0 is different from that of the neighbouring cells for the presence of a lid about 50 km thick and with a V_s of about 4.5 km/s. Going towards the South, the Moho in cells a1-a5 falls in the depth range from 26 to 42 km. A mantle wedge is seen in cells a1-a3. It is characterized by variable V_s, in the range 3.95-4.15 km/s, and its thickness (about 10 km in cell a3) increases going towards west (about 45 km). Cell a3 is characterized by the thinnest mantle wedge (with a percentage of partial melting of about 2-3%, accordingly with BOTTINGA & STEINMETZ, 1979) of this northernmost study area and it could be associated to the inactive recent volcano of Roccamonfina; similarly the low velocity layer of cell a2 (with a percentage of partial melting less than 2%) can be correlated with the inactive volcanoes of Albani Hills. In cell a4 a relatively low velocity layer is also present, with V_s around 4.2 km/s, and less than 10 km thick. A high velocity layer ($4.65 \leq V_s \leq 4.80$ km/s) is surmounted by the mantle wedge layer in cells a1-a4 and its thickness varies from about 35 km to 100 km. Cell a5, on the contrary, has the uppermost mantle structure rather similar to that of cell b3.

Cell A1 mimics the structure geometry of cell a1, but with a lower velocity both for the mantle wedge (V_s around 4.05 km/s) and the layer below it (V_s about 4.5 km/s). Similarly, cells A5 and A6 well resemble the structural characteristics of the uppermost mantle of cells a4 and a5, respectively, but with the lowermost lid at a velocity of about 4.6 km/s and reaching a depth of about 130-170 km.

In the central area of the Tyrrhenian Sea study area (cells A2, A3 and B1-B4), the average Moho is very shallow (about 7 km deep) and the lid thickness is less than about 15 km. Below this thin and strongly laterally variable lid (V_s in the range 4.0-4.4 km/s), there is a very well developed low velocity layer (V_s in the range 2.90-3.85 km/s) with variable thickness (in the range 8-33 km) and centred at a depth of about 20 km (uppermost asthenosphere). A similar layering is found in the uppermost 30 km of cell A4, the main difference being a deeper Moho, at a depth of about 15 km.

The V_s in the uppermost upper mantle of cells A2-A4 and B1-B4 is consistent with a high percentage of partial melting (about 10% accordingly with BOTTINGA & STEINMETZ, 1979). This regional feature, in cells B1-B4, is well compatible with the presence of anomalous shallow mantle materials reported by TRUA *et alii* (2002) in correspondence of the huge volcanic structures like the Vavilov-Magnaghi and the Marsili Seamounts; the shallow partial melting in cells A3 and A4 can be associated to Ischia, Phlegraean Fields and Vesuvio active volcanoes.

In cells A2-A4 the top of the high velocity lid (V_s about 4.45-4.55 km/s) is at a depth of about 30-40 km. In the other cells (B1-B3), the V_s just below the very low velocity layer in the uppermost asthenosphere, is in the range 4.10-4.15 km/s. In cell B4, the asthenosphere is perturbed by a layer with relatively high velocity (V_s about 4.4 km/s) and centred at a depth of about 120 km.

Going towards East (cells B5-B6) the Moho is as deep as about 27-33 km. In B5 the lid velocity increases with increasing depth and the lithosphere is about 110 km thick; in cells B6 the lid is characterized by high V_s and reaches depths of about 100 km.

The structural models of cells C1-C5 (fig. 2b) are markedly different from those of cells B1-B4. In fact, the Moho depth varies from about 13 km to 34 km and the smaller value is reached in correspondence of the active Aeolian volcanic islands (cells C4 and C5). In cells C2-C3 the V_s gradient in the lid, which is about 70-90 km thick, is stronger than the gradient that characterizes the sub-Moho materials in cell C1. In C4, the V_s immediately below the Moho can be as low as 3.85 km/s (about 3-4% of partial melting, accordingly with BOTTINGA & STEINMETZ, 1979), while the high velocity lid is found at a depth larger than about 40 km. In C5 the relatively soft lid extends only to about 17 km of depth and it is on top of a low velocity (V_s about 3.5 km/s) layer, the mantle wedge (about 10% of partial melting, accordingly with BOTTINGA & STEINMETZ, 1979), which overlies a lithospheric root (V_s around 4.6 km/s) reaching about 140 km of depth. The large amount of partial melting (where V_s in the upper mantle is less than 4.0 km/s) in C4 and C5 correlates well with the presence of the Aeolian volcanic islands (Lipari and Vulcano in C4 and Stromboli in C5).

The structural properties change abruptly in cell C6. Below a crust about 25 km thick, and a very thin lid, there is a low velocity (V_s around 3.6 km/s) layer about 10 km thick, on top of a layer with V_s around 4.6 km/s that reaches a depth of about 100 km. These features (not imposed a priori in the inversion scheme) can be interpreted as a lithospheric doubling and the deeper Moho can be seen about 38 km deep.

In Sicily, cells D1-D4 (fig. 2b) show a Moho that deepens from West to East from about 25 km to 35 km, while in the Etna area (cell D5) the Moho is only about 23 km deep. In cells D1-D2 the lid thickness varies between 80 km and 40 km and the V_s increases with increasing depth, about 4.20-4.65 km/s. Cells D3 and D4 have a high velocity lid with V_s 4.65 km/s, reaching a depth of about 90 km.

In cells C5 and C6, below the high velocity lid of about 4.60 km/s, there is a layer characterized by a V_s around 4.25 km/s. PANZA *et alii* (2003) suggest that the structural setting depicted by the models for cells C5-C6 and the area East of them indicate the subduction of a rifted continental Ionian lithosphere, formed during the Jurassic extensional phase.

In cell D5 a mantle wedge (V_s about 4.1 km/s) is detected just below the Moho and it overlies a high velocity lid (V_s about 4.5 km/s) that reaches the velocity of 4.8 km/s and the depth of about 160 km. The V_s around 4.1 km/s implies that, in the mantle wedge, the partial melting is around 1-2% (BOTTINGA & STEINMETZ, 1979).

3.3. - THE ASTHENOSPHERE.

The properties below the uppermost upper mantle change significantly going from Sicily, through the Tyrrhenian Sea and towards the Apennines. In fact, the depth of the top of the asthenosphere is very variable and its bottom is not always detected at about 200-250 km of depth.

In c0-c2 (fig. 2a) the asthenosphere has a V_s of about 4.3-4.4 km/s, and it starts at a depth of about 170 km in c1-c2 and of about 70 km in c0. Cells c3 and b0-b3 are characterized by an asthenosphere with V_s varying in the range 4.00-4.25 km/s whose top is at the depth of about 80 km in b0 and between 135-160 in b1-b3 and c3. The estimated thickness of the asthenosphere is about 100 km in c3, b0, b2 and 70 km in b1, and not detectable in b3 (as in the cells c0-c2). In cells b1-b2 and a1-a4, the shallow mantle wedge is separated from the asthenosphere by a high velocity lid, very variable in thickness. In cells b1 and a1 the asthenosphere is only about 60-70 km thick and centred at an average depth of about 160 km. In b2 it

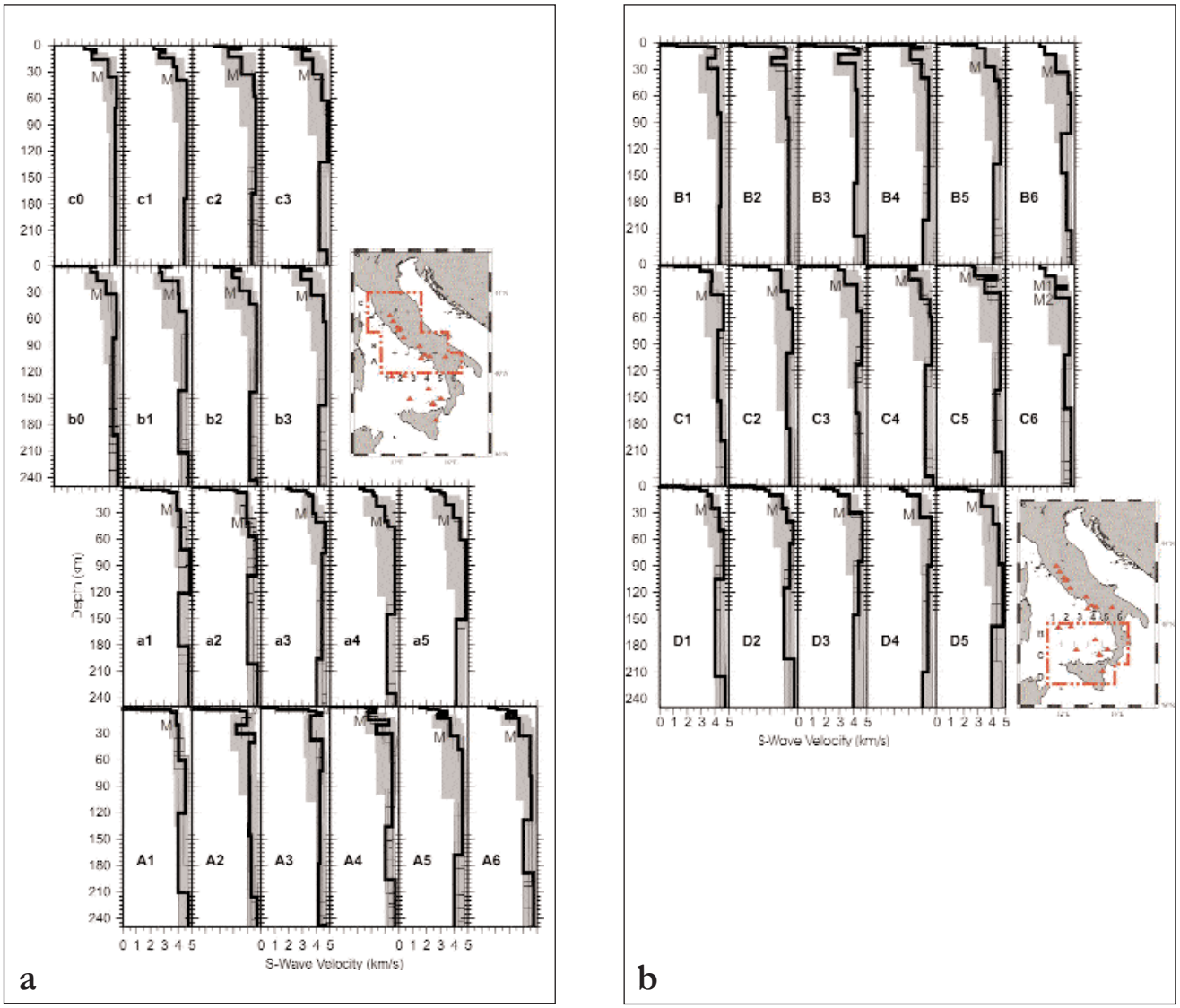

Fig. 2. - *(a and b) The set of solutions (thin lines) obtained through the non–linear inversion of the dispersion relations of each cell in the evidenced area (indicated in the insert). The investigated parameter's space (grey zone) and the chosen solution (bold line) are shown as well. The Moho is marked with M. M1 and M2, in cell C6, indicate the lithospheric doubling.*

is deep as in b1 and has a thickness of about 100 km. In cell A1 the asthenosphere, with V_s around 4.0 km/s, starts around the depth of 120 km and ends at the depth of about 210 km. Going from cell a2 to cell a5, the asthenospheric layer is very different. In cell a2 the top of the asthenosphere is at a depth of about 100 km, with a thickness of about 100 km. The asthenospheric V_s in a3 ranges from 4.4 km/s to 4.0 km/s. Finally, in a4-a5 the asthenosphere is characterized by V_s around 4.2 km/s and in a5 it reaches a depth larger than 250 km.

In the central part of the Tyrrhenian Sea study area, the asthenosphere is as shallow as about 10 km and, between the Tyrrhenian and Ionian basins (see PANZA *et alii*, 2003), the asthenosphere is interrupted by a seismogenic high velocity body dipping towards NW (cells C5 and C6, fig. 2b).

In cells A2-A4 the high velocity lid is surmounted by a mantle wedge (V_s about 3.35-4.25 km/s) originally detected by CALCAGNILE & PANZA (1981), PANZA *et alii* (1980) and confirmed by the geochemical analysis of LOCARDI (1986). A similar situation is seen in cells C4 and C5, where the V_s in the wedge is in the range 3.50-4.35 km/s. In the cells, A2-A3 and B1-B3, V_s reaches the maximum velocity of about 4.35 km/s in the lower asthenosphere. The lower bound of the asthenosphere is at a depth of about 215 km in A2 and B3, 245 km in A3 and deeper than 250 km in B1-B2. In cells A4-A6 the asthenosphere is very pronounced (V_s about 4.0 km/s), it starts at a depth variable in the range from 130 to 170 km and reaches the depth of about 190 km in A4 and A6 and larger

than 250 km in A5. In cells A4 and A5, the relatively low velocity layer could have the same origin as in cells C5 and C6.

In B4, where the asthenosphere is perturbed by a layer with relatively high velocity at about 4.4 km/s, and B5 the V_s at the low velocity asthenospheric layer varies in the range 4.00-4.10 km/s and the bottom of the low velocity layer reaches a depth larger than 250 km.

In A6 and B6 the asthenosphere starts at a depth of about 130 km and 100 km, respectively, and extends for 60-100 km with V_s about 4.0 km/s in A6 and ranging from 4.0 km/s to 4.4 km/s in B6. In cells C1-C4, going towards East, the asthenosphere is as deep as about 75 km reaching a maximum depth of about 115 km. The V_s is in the range 4.20-4.40 km/s in C1-C3 and is about 4.20 km/s in C4, with the bottom of the low velocity layer detectable at depth exceeding 200 km only in C1 and C4. The cells C6 and C5 are characterized by a low velocity layer about 60-70 km thick and with V_s about 4.25 km/s, deeper in C5 than in C6. The asthenospheric low velocity layer is well developed in cells D1-D5 (with the minimum V_s about 4.0 km/s) with the top varying in the depth range from 65 to160 km. In D5 a relatively high velocity body (V_s in the range 4.5-4.8 km/s) separates the asthenosphere from the shallow mantle wedge with V_s around 4.10 km/s.

4. - PETROLOGICAL DATA AND METHOD

The study of primary (i.e., not modified by evolution processes) or near-primary magmatic rocks is able to furnish a wealth of information on the composition of their source zones. Since basaltic magmas come from the upper mantle, their study can provide important information on mantle composition and evolution.

The major element composition of primary magmas depends on the type and proportion of the phases that enter into the melt during anatexis. This can be better understood by the use of phase diagrams, which can be constructed either experimentally or on the basis of free energy values of various phases at different P-T conditions. Phase diagrams are able to furnish information on the stability fields of mineral phases, the proportions of the phases that enter into the melt, the major element composition and the degree of silica saturation of the melts, and the modification of melt compositions with changing degrees of anatexis.

Trace elements give additional and complementary information on melt composition and their source. The equation that describes the variation of trace elements during equilibrium batch melting is:

$$C_l/C_0 = 1/(D(1-F)+F) \quad (1)$$

where Cl is the concentration of a given trace element in the magma, C0 is the concentration of the same element in the source rock, D (partition coefficient) is the ratio between the abundance of the element in the residual minerals and in the coexisting melt; F is the degree of partial melting.

Some elements, known as *incompatible,* strongly prefer to enter the liquid phase during partial melting (i.e. D~0). For the mantle rocks, incompatible elements include Th, U, Ta, Nb, Rb, Ba, Light Rare Earth Elements (LREE), Zr, etc. When D = 0 equation (1) becomes:

$$C_l/C_0 \sim 1/F \quad (2)$$

Equations (1) and (2) demonstrate that the concentration of an incompatible element in the magma depends on the concentration of the element in the source rock, and increases with decreasing degrees of partial melting.

However, ratios of incompatible elements are largely independent of the degrees of partial melting and reflect source composition. Therefore, different ratios of highly incompatible elements in basaltic magmas suggest distinct values for the source rocks. These, in turn, reveal different evolutionary histories of the mantle sources. Study of incompatible element ratios in mantle-derived magmas is helpful for reconstructing the nature of these modifications.

The isotopic ratios of several elements (e.g. $^{87}Sr/^{86}Sr$, $^{143}Nd/^{144}Nd$, $^{206}Pb/^{204}Pb$, $^{207}Pb/^{204}Pb$, $^{208}Pb/^{204}Pb$, $^{16}O/^{18}O$) are not significantly modified during equilibrium partial melting; primary magmas inherit the isotope signatures of their sources. Therefore, isotope composition of basaltic rocks is of key importance to understand the composition and evolution of mantle rocks.

One of the main problems in investigating the mantle composition, through the study of basaltic rocks, is that magmas erupted at the surface rarely represent unmodified primary melts. In most cases, they undergo geochemical diversification by fractional crystallisation, assimilation, and mixing, or, more commonly, by a combination of these processes. However, closed-system fractional crystallisation produces strong variations in major and trace element abundances, but leaves incompatible element ratios and isotopic signatures unaffected. On the contrary, assimilation and mixing may generate dramatic modification of the element abundances and ratios, and of the isotope signatures. Therefore, a golden rule for studies of mantle compositions through studies of the magmatism is to focus on the most primitive rocks

(e.g. those with the highest Ni, Cr, MgO and Mg# = Mg/(Mg+Fe^{+2}) atomic ratio). Primary mantle-equilibrated magmas have Mg# around 70, Ni = 250-300 ppm and Cr = 500-600 ppm. Therefore, basalts with high Mg#, Ni and Cr are the closest representatives of their mantle-equilibrated parents and furnish the maximum of information on mantle composition and processes.

5. - REGIONAL LITHOSPHERIC MODELS FROM PETROLOGICAL-GEOCHEMICAL DATA

Petrological and geochemical data of mafic rocks can be used to place constraints on the composition of the upper mantle beneath the Italian Peninsula and the Tyrrhenian see floor. Figure 3 is a classification diagram based on ΔQ vs. K_2O/Na_2O relationships (PECCERILLO, 2001a). ΔQ is the algebraic sum of normative quartz (Q), minus nepheline (ne), leucite (lc), kalsilite (ks) and forsterite; it measures the degree of silica saturation of magmas: ΔQ<0 means undersaturated magmas, whereas ΔQ>0 reveals silica oversaturated magmas.

It can be noticed that the Italian mafic volcanics range from tholeiitic and calcalkaline to Na-alkaline, shoshonitic, potassic and ultrapotassic. This is a strong regional variation of magma types. For instance, Na-alkaline rocks occur in Sicily; calcalkaline and shoshonitic rocks are concentrated in the Aeolian arc; potassic and ultrapotassic rocks represent the main magma types along the Italian peninsula. However, the potassic and ultrapotassic rocks from Umbria and Tuscany have different composition than other K-rich rocks from central Italy, and the Vulture rocks are strongly undersaturated in silica and have variable K_2O/Na_2O ratios.

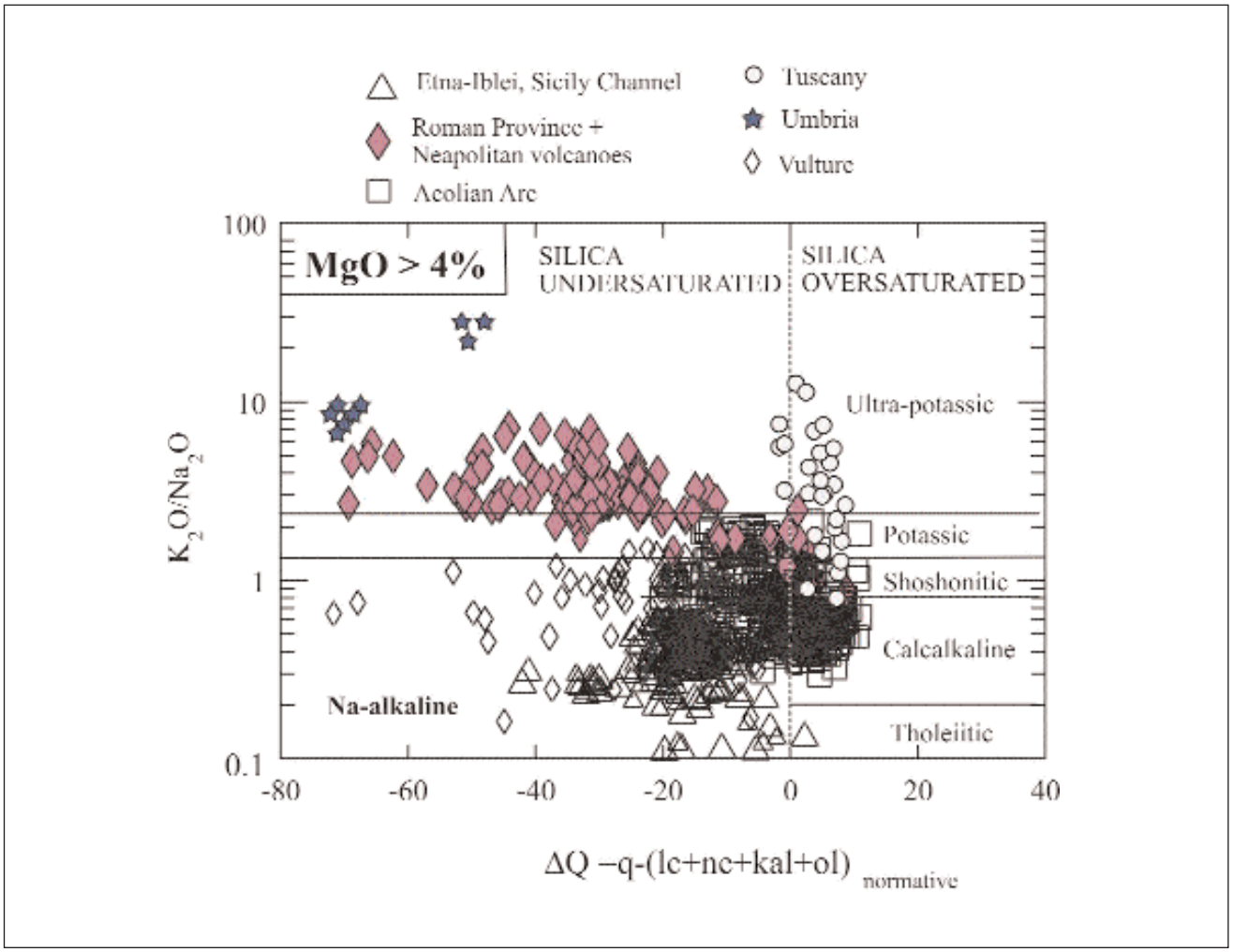

Fig. 3. - *Classification diagram based on ΔQ vs. K2O/Na2O for Plio-Quaternary mafic rocks (MgO > 4 wt%) from Italy. ΔQ is the algebraic sum of normative quartz (Q), minus leucite (lc), nepheline (ne), kalsilite (kal) and olivine (ol); it measures the degree of silica saturation of rocks. Silica oversaturated rocks have ΔQ> 0, whereas silica undersaturated rocks have ΔQ < 0. Modified after* PECCERILLO (2001a).

Other differences among various potassic rocks are found for Na_2O, Al_2O_3, CaO concentrations. Tuscany ultrapotassic rocks are depleted in Na_2O, CaO and Al_2O_3: this particular type of ultrapotassic rocks are known as *lamproites*. The rocks from Umbria are low in Na_2O and Al_2O_3 but have high CaO: these ultrapotassic rocks are known as ultrapotassic *kamafugites* (PECCERILLO *et alii*, 1988).

Most mafic rocks in Italy have higher Na_2O, Al_2O_3, CaO than lamproites, and variable potassium contents. These rocks are known as Roman-type potassic (KS) and ultrapotassic (HKS) rocks (FOLEY *et alii*, 1987). KS rocks are moderately rich in potassium and are nearly saturated in silica; HKS rocks have $K_2O > 3$ and $K_2O/Na_2O > 2.5$, and are strongly undersaturated in silica. KS and HKS form the large volcanic complexes of Vulsini, Vico, Sabatini and Alban Hills, the Ernici and Roccamfonfina centres, and the Campania volcanoes (i.e. Ischia, Vesuvio and Phlegraean Fields).

Major elements and the degree of silica saturation give important clues as to the genesis of the various groups of Italian mafic rocks. The low Ca, Na and Al of lamproites indicate a generation in an upper mantle that was depleted in Ca- and Na- bearing phases such as clinopyroxene. Therefore, a harzburgite source, i.e. a rock mainly formed of orthopyroxene and olivine, is inferred for lamproites. The silica oversaturated nature of lamproitic magmas suggests melting at low pressure (FOLEY, 1992). However, the high K_2O content of these rocks require a K-rich phase (e.g., phlogopite, pargasite) in the mantle. In summary, lamproites reveal the occurrence of a phlogopite-rich harzburgitic mantle at low pressure beneath southern Tuscany.

The high CaO of kamafugites require abundant clinopyroxene; moreover, high K points to phlogopite bearing upper mantle. Therefore, the kamafugite source may be represented by a phlogopyre clinopyroxenite. Kamafugites occur in Umbria, and this points to the presence of clinopyroxenite upper mantle beneath this region.

The high Al, Ca, K, and Na of Roman-type rocks suggest that mantle sources were represented by a phlogopite- clinopyroxene- bearing peridotite. The variable enrichment in potassium of KS and HKS likely relates to different degrees of partial melting and/or to a variable quantity of phlogopite in the mantle.

A particular type of alkaline rocks, rich in both Na and K, occur at Mount Vulture (DE FINO *et alii*, 1986). High alkalis make the rocks in this volcano distinct from any other potassic rocks from central-southern Italy. However, the origin of these rocks is still poorly understood.

The calcalkaline and shoshonitic rocks have comparable Al, Ca and Na contents as the Roman-type rocks, but display comparable to lower potassium contents. The major element chemistry suggests a genesis in lherzolitic sources, but with low amounts of potassium-rich phases. Moreover, the CA magmas require hydrous conditions during partial melting (e.g. WENDLANDT & EGGLER, 1980). Therefore, petrological data suggest the presence of a hydrated lherzolitic upper mantle beneath the Aeolian arc.

Thus, the major element data suggest that the volcanism of central southern Italy has been generated in petrologically heterogeneous mantle sources. Since various types of magmas are concentrated in different regions, the obvious implication is that the upper mantle beneath Italy is a mosaic of mineralogically different peridotitic rocks.

Trace element and isotope geochemistry can furnish additional constraints on the nature of the upper mantle beneath Italy. Variations of key incompatible element ratios and isotopes are shown in figure 4 and figure 5.

It can be noticed that mafic rocks from various volcanic areas define different trends or plot in different areas, which calls for geochemically different mantle sources. In particular, it can be noted that the volcanic rocks from Naples area plot in the same field as Stromboli. These rocks show strong compositional differences as Tuscany and Roman areas. Moreover, the rocks from Roccamonfina and Ernici Mts. partially plot with Neapolitan volcanoes and partly with Roman volcanics. Therefore, the Ernici Mts.-Roccamonfina region is characterised by the coexistence of two geochemically and isotopically distinct rocks suites.

In conclusion, major element, trace element and isotopic data on mafic rocks suggest that Italian volcanism can be subdivided into different magmatic provinces, which were generated by petrologically and geochemically distinct mantle sources. These zones are shown in figure 6 (PECCERILLO, 1999; PECCERILLO & PANZA, 1999).

5.1. - SOUTHERN TUSCANY PROVINCE

The province extends from southern Tuscany and the Tuscan archipelago to the Tolfa-Manziana zone. It is formed by an association of mantle-derived mafic magmas and crustal anatectic acid rocks. Mafic rocks have variable enrichment in potassium, but have peculiar incompatible trace element ratios and isotope signatures. Lamproitic rocks occur in this region, which suggest a phlogopite-bearing harzburgitic upper mantle at low pressure. All the mafic rocks have crustal-like isotopic signatures (e.g., $^{87}Sr/^{86}Sr$ around 0.712-0.717; POLI *et alii*, 1984; CONTICELLI & PECCERILLO, 1992; CONTICELLI *et alii*, 2001). Acid crustal anatectic intrusive and effusive rocks (e.g. Roccastrada, Elba, etc.) associated with mafic magmas are likely related to intra-crustal anatexis induced by isotherm uprise during mafic magma emplacement.

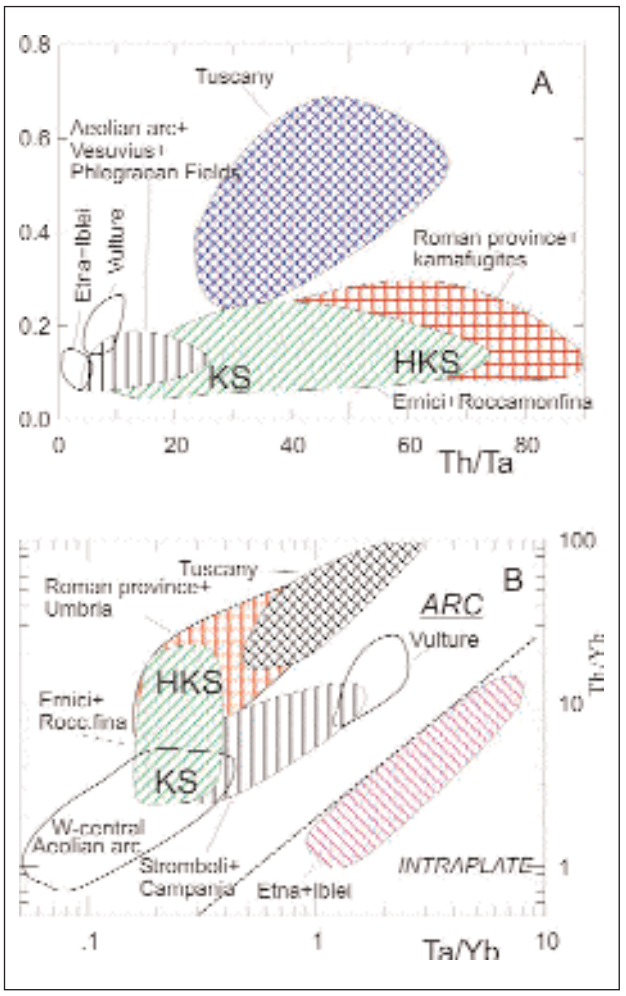

Fig. 4. - *Variation of trace element ratios in the Plio-Quaternary mafic rocks (MgO > 4 wt%) from Italy. Note that: 1) rocks from the various zones plot in different fields; 2) Stromboli and Neapolitan volcanoes plot along the same trend; 3) the Ernici and Roccamonfina potassic rocks (KS) plot with Campania-Stromboli, whereas ultrapotassic rocks (HKS) plot in the filed of the Roman Province.*

5.2. - Roman Province s.s.

The province includes the Vulsini Mts., Vico, Sabatini and the Alban Hills. It is formed by KS and HKS rocks with variable degree of evolution. Trace element ratios are different from those of Tuscany rocks; moreover isotope compositions are less extreme than in Tuscany (e.g. $^{87}Sr/^{86}Sr$ is typically around 0.710; e.g., Conticelli & Peccerillo, 1992). The high CaO, Al_2O_3, Na_2O and K_2O contents of Roman province reveal the presence of phlogopite-bearing lherzolitic mantle sources beneath the Roman area.

5.3. - Umbria province

The province is formed by kamafugitic rocks, which have incompatible element ratios and isotopic signatures similar as those of the Roman province. However, the low Na and Al and the very high CaO and K_2O suggest the presence of a phlogopite-clinopyroxenite mantle source for these magmas, which is distinct from the Roman province.

5.4. - Ernici-Roccamonfina

The province consists of potassic and ultrapotassic (KS and HKS) rocks that display distinct enrichment in potassium and incompatible elements, and isotopic signatures. KS rocks are similar to Neapolitan volcanoes and Stromboli, whereas HKS resemble Roman rocks. This testifies to the occurrence of a compositionally zoned upper mantle beneath Ernici-Roccamonfina, which is peculiar of this area.

5.5 - Campania Province- Stromboli

Campania volcanoes are represented by the active volcanoes of Naples area (Vesuvio, Phlegraean Fields and Ischia) and by slightly older volcanic rocks found by borehole drilling (Di Girolamo, 1978). Stromboli consists of calcalkaline, shoshonitic and potassic rocks, which show strong compositional similarities with the Campanian volcanoes (Peccerillo, 2001b). However Vesuvio shows an ultrapotassic composition, which is not found at Stromboli, Ischia and Phlegraean Fields.

5.6. - Aeolian arc.

Two sectors can be distinguished in the Aeolian arc. The western Aeolian arc basically consists of CA volcanics with low $^{87}Sr/^{86}Sr$ (= 0.7035-0,7045). The eastern sector (Panarea and Stromboli) consists of calcalkaline to KS rocks with Sr isotope ratios of about 0.704 to 0.707 (i.e. from the low values typical of the western arc to those typical of Campania volcanoes; De Astis *et alii*, 2000).

5.7. - Mount Vulture

The alkaline rocks are enriched in both Na and K, and hauyne rather than leucite is the most typical feldspathoidal mineral. Vulture rocks have major and trace element composition that is distinct from other Italian volcanics, which indicates a different mantle source

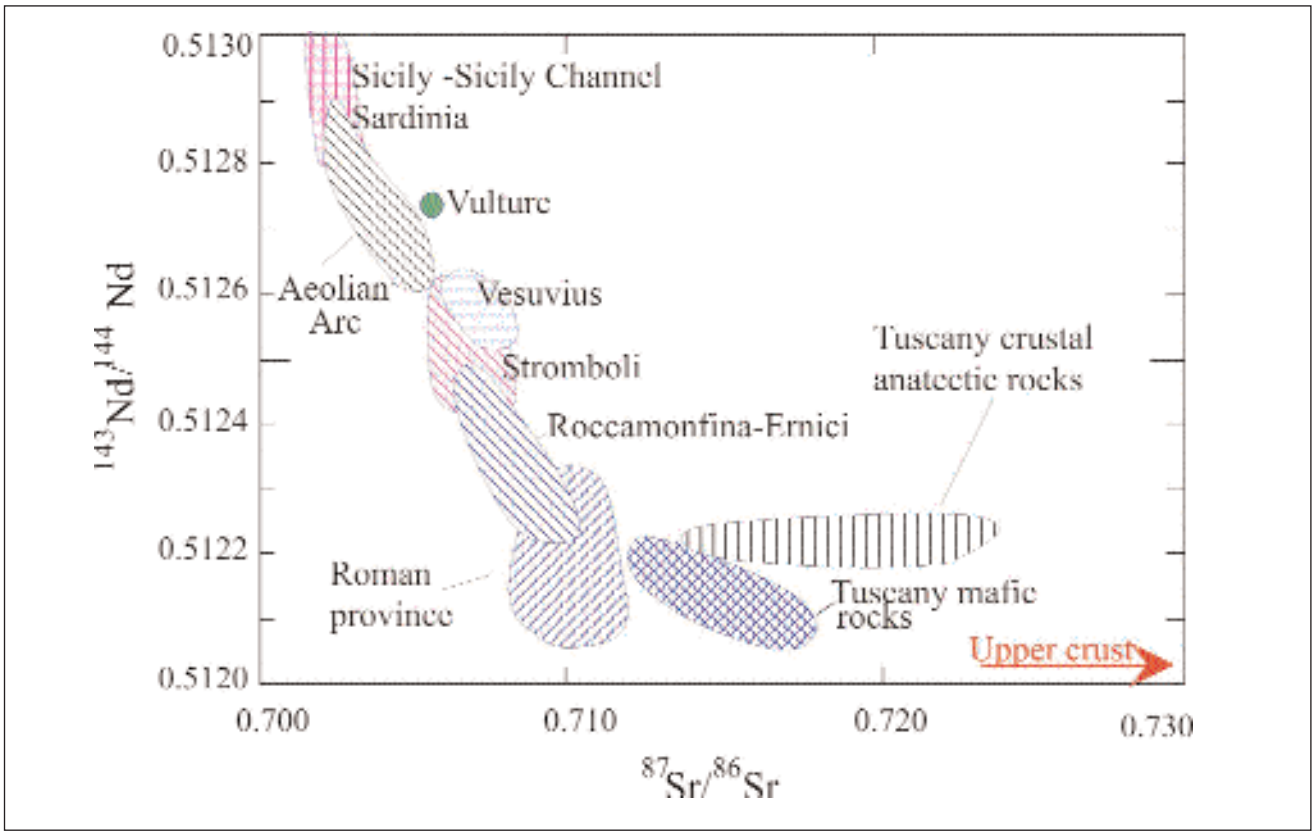

Fig. 5. - *Plot of $^{87}Sr/^{86}Sr$ vs. $^{143}Nd/^{144}Nd$ in the Plio-Quaternary mafic rocks (MgO > 4 wt%) from Italy.*

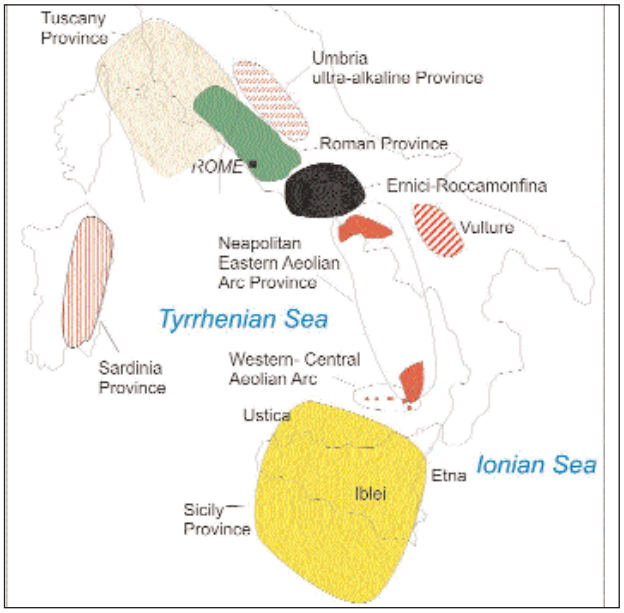

Fig. 6. - *Plio-Quaternary magmatic provinces in Italy. Modified after* Peccerillo & Panza (1999).

5.8. - Sicily Province

The province consists of tholeiitic and Na-alkaline rocks (Etna, Iblei, Sicily Channel) with distinct trace element and isotopic composition as the other provinces. All these centres display typical intraplate geochemical affinity.

5.9. - Tyrrhenian Sea

A large volume of volcanic rocks are hidden below the Tyrrhenian Sea. The few data available on the Tyrrhenian seamounts indicate a compositional variability. Tholeiitic rocks seem to prevail among the younger products. Ages range from Miocene to Pliocene and increase in age going westward toward the Oligocene-Miocene calcalkaline and shoshonitic belt of Sardinia. This magmatism is the result of the SE migration of subduction processes and of asthenospheric mantle uprise behind the volcanic arc (e.g. Beccaluva *et alii*, 1989; Locardi, 1988 and 1993; Locardi & Nicolich, 1988).

6. - THE MODELS TYING PETROLOGICAL AND GEOPHYSICAL DATA

In figure 7 the selected solutions for the 10x10 cells containing recent volcanism are shown. On the base of the discussed data it is possible to recognize the following groups:

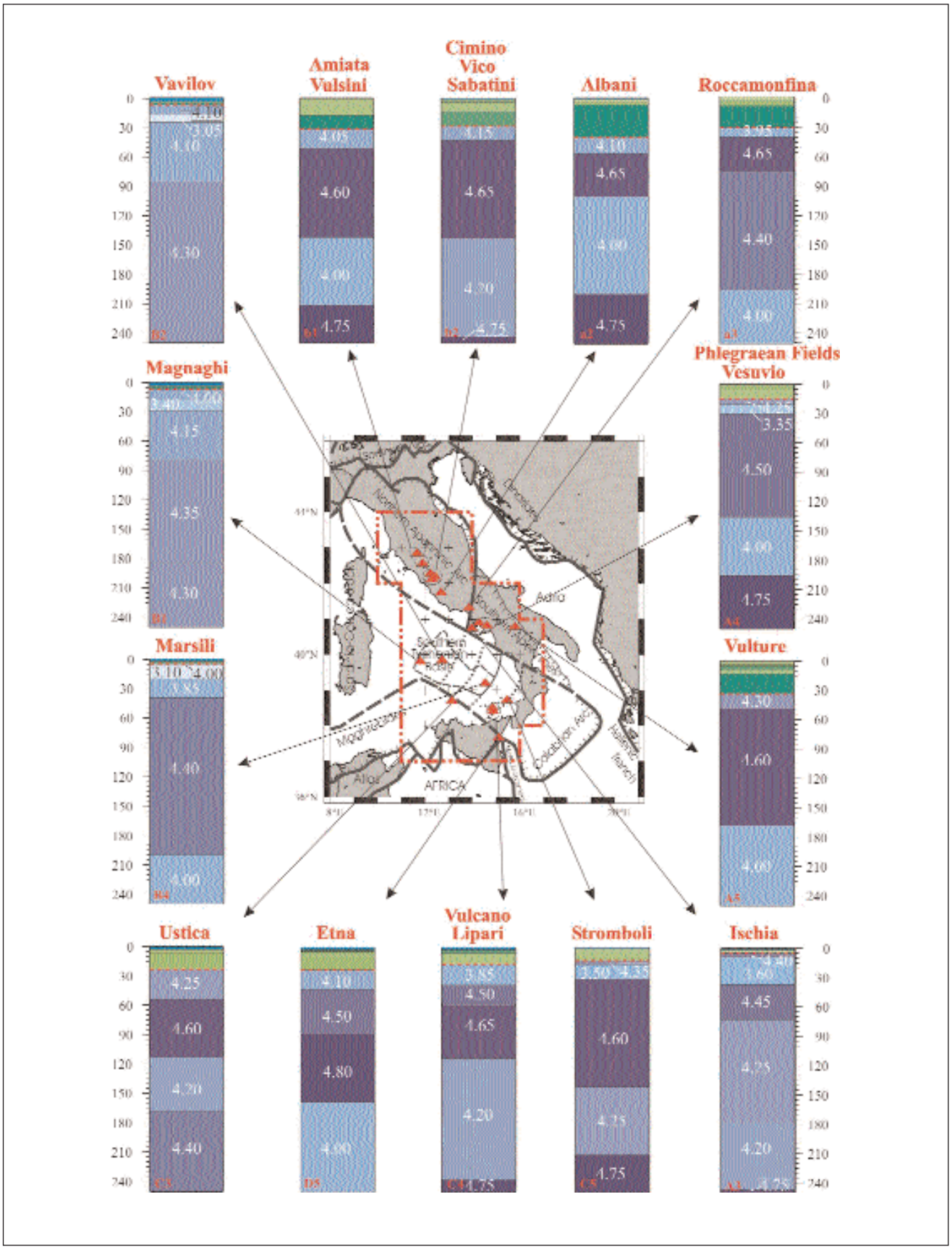

Fig. 7. - *The chosen structure (the solution of each set indicated by bold line in fig. 2) of the cells (indicated in red) containing the recent volcanoes (indicated by red triangles in the central frame): Amiata-Vulsini (b1), Cimino-Vico-Sabatini (b2), Albani (a2), Roccamonfina (a3), Phlegraean Fields-Vesuvio (A4), Vulture (A5), Ischia (A3), Stromboli (C5), Vulcano-Lipari (C4), Etna (D5), Ustica (C3), Marsili (B4), Magnaghi (B1), Vavilov (B2).*

6.1. - Magnaghi, Vavilov and Marsili

Magnaghi, Vavilov and Marsili are characterized by a thin crust sitting on a very thin lid bounding a very low velocity layer in the mantle. This low velocity in the uppermost mantle can be interpreted as the indication of the existence of large amounts of melt. These seamounts represent back arc volcanoes with a dominant tholeitic petrochemical affinity, which requires a genesis at low pressure by high degree (some 10%) of partial melting in the mantle. Therefore this uppermost mantle low velocity layer seems to be the source of the back arc volcanism in the Tyrrhenian.

6.2. – Ustica, Etna and Vulture

Ustica, Etna and Vulture are characterized by a continental crust with thickness variable from about 23 to about 33 km, that overlies a mantle whose uppermost part, up to a depth of about 50 km, has V_s in the range from about 4.1 km/s (Etna) to about 4.3 km/s (Vulture); below this layer, the lid (V_s about 4.5-4.8 km/s) extends to depths between 115-170 km. The three volcanoes have variable geochemical signatures. Etna and Ustica have Na-alkaline affinity, similar trace elements and Sr isotopic compositions, which fall in the range of the intraplate volcanoes, even if evidence for a subduction related geochemical component has been found (Cristofolini *et alii*, 1987; Cinque *et alii*, 1988). The Vulture volcano results from the interaction between intraplate and subduction related reservoirs, but the subduction component is much stronger that at Etna and Ustica. In spite of the variable petrological, geochemical and isotopic signatures, subduction and intraplate components have played a role in the genesis of these volcanoes. The unifying elements of these volcanoes are: (a) their lateral position with respect to the active subduction, (b) the coexistence of subduction and intraplate related geochemical signatures, (c) similar structure of the lithosphere-asthenosphere system. Thus, the structure of the magma sources and the geochemical signatures could be related to the contamination of the side intraplate mantle by material coming from the either active (the case of Etna) or ancient (the cases of Ustica and Vulture) roll back.

6.3. – Stromboli, Phlegraean Fields and Vesuvio

Stromboli, Phlegraean Fields and Vesuvio are characterized by a thin continental crust (about 15 km thick). Below the crust there is a mantle wedge with V_s as low as about 3.35-3.50 km/sec in its deeper part and about 4.25-4.35 km/s just below the Moho (the lid). In correspondence of the Phlegraean Fields and Vesuvio, the layering under the wedge is consistent with the presence of a subducted lithospheric slab (Ionian/Adria slab), seismically active at depth larger than 300 km, and the crust contains a well developed low velocity layer, about 10 km thick and centred at a depth of about 10 km. The strong similarity in the geochemical and isotopic composition between Stromboli and Phlegraean Fields and Vesuvio matches well the similarity in the lithospheric structural models. The anomalous K enrichment in Vesuvio magmas could be a feature acquired either by melting of higher proportion of a K-rich phase or may be related to low pressure magma evolution.

6.4. – Vulcano and Lipari

Vulcano and Lipari are in a thin continental crust, less than 20 km thick, that overlies a very soft upper mantle (V_s ~ 3.85 km/s). In the mantle the V_s reaches about 4.65 km/sec and about 115 km of depth. This lithospheric structural setting has relevant affinities with the models described for Etna and Ustica rather than to the one of the nearby Stromboli. The structural difference between Vulcano and Stromboli lithosphere is not surprising considering the different geochemical signatures. On the other side, the affinity between Vulcano, Lipari and Etna could be explained by the common position along the Tindari-Letoianni-Malta fault zone. The clear difference in V_s distribution, between the Eastern (Stromboli) and the Central-Western (Vulcano and Lipari) sectors of the arc, could have been partly masked by a different positioning of the 10x10 cells, therefore the geochemical data are a strong support for our findings. Zanon *et alii* (2003), Frezzotti *et alii* (2003), in their model of the Vulcano island and Aeolian arc magmatic evolution, suggest the existence of a deep accumulation reservoir, at about 18-21 km, and of a shallow accumulation level in the upper crust, at a depths of 1.5-5.5 km. Petrological and geochemical data of Gauthier & Condomines (1999), Francalanci *et alii* (1999) show that the magma of the volcano has properties that are characteristic of magma chambers located at different depths. It is possible to associate the layer with V_s at about 3.85 km/sec, just below the Moho, to the deepest magma reservoir found by Zanon *et alii* (2003), Frezzotti *et alii* (2003), while the resolution of our data does not allow us to sort out the uppermost (crustal) accumulation zone.

6.5. – Ischia

Ischia is geochemically and petrologically belonging to the other Campanian volcanoes. Therefore the quite remarkable difference in the structural lithospheric

model, with respect to the Phlegraean Fields and Vesuvio, could be partly related to the resolving power of our geophysical data and, however, it could reveal a transition to the Tyrrhenian domain.

6.6. – Amiata, Vulsini, Cimino, Vico, Sabatini, Albani, Roccamonfina

Amiata, Vulsini, Cimino, Vico, Sabatini, Albani, Roccamonfina sit on a continental crust about 30 km thick (40 km for Albani) and the V_s below the Moho is rather low (in the range 3.95-4.15 km/sec). The main differences are seen below the high velocity lid (about 4.6 km/s). The asthenospheric "low" velocity layer (V_s < 4.4 km/s) is very deep (it starts at about 200 km of depth) under Roccamonfina, while it is about 145 km deep in Cimino-Vico-Sabatini and Amiata-Vulsini, and 100 km deep in Albani. The region from Vulsini to Albani Hills is rather homogenous from a petrological point of view, being mainly formed by ultrapotassic rocks with poorly variable geochemical and isotopic signatures. On the other side, the Roccamonfina area differs significantly form the northern Latium volcanoes because of the occurrence of both potassic and ultrapotassic rocks with very distinct geochemical and isotopic compositions. Also in this case the differentiation of the provinces of Roccamonfina and Latium finds a correspondence in the upper mantle structure.

7. - CONCLUSIONS

In the Tyrrhenian Sea area, large-scale inhomogeneities in the lithosphere-asthenosphere structure are reflected by large variations in the composition of magma types.

The main features identified by our geophysical study are: (1) a low velocity mantle wedge, just below the Moho, as the common feature detected in all the cells containing inactive recent volcanoes (Amiata, Vulsini, and Cimino, Vico, Sabatini, Albani Hills and Roccamonfina) in the Tuscany and Roman regions; (2) a very thick rigid body in the upper mantle beneath the Ernici-Roccamonfina province that exhibits a distinct geochemical and isotopic compositions when compared with the Roman province; (3) a shallow and very low V_s layer in the mantle in the areas of Aeolian islands, Vesuvio, Ischia and Phlegraean Fields, which represents their shallow-mantle magma source; (4) a very shallow crust-mantle transition in the Southern Tyrrhenian Sea and very low V_s just below a very thin lid in correspondence of the submarine volcanic bodies (Magnaghi, Marsili & Vavilov); (5) a shallow mantle wedge, below Etna's crust, consistent with the hypothesis of the presence of an asthenospheric window feeding the volcano; (6) the subduction of the Ionian lithosphere towards NW below the Tyrrhenian Basin; (7) the subduction of the Adriatic/Ionian lithosphere underneath the Vesuvio and Phlegraean Fields.

Petrology and geochemistry reveal rocks ranging in composition from tholeiitic to calcalkaline to sodium- and potassium-alkaline and ultra-alkaline. Scrutiny of the relevant data allows us to recognize several magmatic provinces, which display distinct major and/or trace element and/or radiogenic isotope signatures: Tuscany, Latium (Roman Province), Umbria (kamafugitic province), Ernici-Roccamonfina, Campania Province, Stromboli, Vulture, Aeolian arc, Sicily and Sicily Channel, Tyrrhenian Sea and Sardinia. The rocks from the Aeolian arc and the Italian Peninsula range from calcalkaline to ultrapotassic, and display trace element ratios (e.g., Th/Ta, La/Nb etc.), which fall into the field of subduction-related (i.e., orogenic) magmatic suites. On the contrary, Sicily, the Sicily Channel and Sardinia rocks have intraplate, (anorogenic) geochemical characteristics.

The combined analysis of petrological, geochemical and geophysical data reveals a surprisingly close match between geophysical characteristics of the lithosphere-asthenosphere and the compositions of magmatic rocks erupted at the surface in the various regions. This suggests that variations of seismic wave velocity in the mantle could be related to compositional modifications of peridotite. The present paper, therefore, provides important constrains that must be considered by geodynamic models for the evolution of the Alpine-Apennines systems.

Aknowledgements

Part of this research is funded by Italian MIUR Cofin *(2001: Subduction and collisional processes in the Central Mediterranean; 2002: A multidisciplinary monitoring and multiscale study of the active deformation in the Northern sector of the Adria plate),* GNDT *(2000: Determinazione dello stile di deformazione e dello stato di sforzo delle macrozone sismogenetiche italiane) and* INGV *(Eruptive Scenarios from Physical Modeling and Experimental Volcanology). The research on Italian magmatism has been funded by* CNR, GNV-INGV *and by the* University of Perugia.

REFERENCES

Ahrens T.J. (1973) - *Petrologic properties of the upper 670 km of the Earth's mantle; geophysical implications.* Phys. Earth Planet. Inter., **7**: 167-186.

Anderson D.L. (2000) - *The thermal state of the upper mantle; no role for mantle plumes.* Geophys. Res. Lett., **27**: 3623-3626.

Bally A.W., Burbi L., Cooper C., & Ghelardoni R. (1986) - *Balanced sections and seismic reflection profiles across the Central Apennines.* Mem. Soc. Geol. It., **35**: 257-310.

Beccaluva L., Macciotta G., Morbidelli L., Serri G. &

TRAVERSA G. (1989) - *Cainozoic tectono-magmatic evolution and inferred mantle sources in the Sardo-Tyrrhenian area*. In: BORIANI A., BONAFEDE M., PICCARDO G.B. & VAI G.B. (Eds.): "*The lithosphere in Italy*". Atti Convegni Lincei, **80**: 229-248.

BISWAS N.N. & KNOPOFF L. (1974) - *The structure of the Upper Mantle under the U.S. from the dispersion of Rayleigh waves*. Geophys. J. R. Astr. Soc., **36**: 515-539.

BOLT B.A. & DORMAN J. (1961) - *Phase and Group velocity of Rayleigh waves in a spherical gravitating earth*. Journal of Geophysical Research, **66**: 2965-2981.

BOTTINGA Y. & STEINMETZ L. (1979) - *A geophysical, geochemical, petrological model of the sub-marine lithosphere*. Tectonophysics, **55**: 311-347.

CALCAGNILE G. & PANZA G.F. (1981) - *The main characteristics of the lithosphere-astenosphere system in Italy and surrounding regions*. Pure Appl. Geophys., **119**: 865-879.

CALCAGNILE G., D'INGEO F., FARRUGIA P. & PANZA G.F. (1982) - *The lithosphere in the central-eastern Mediterranea area*. Pure Appl. Geophys., **120**: 389-406.

CAPUTO M., KNOPOFF L., MANTOVANI E., MUELLER S. & PANZA G.F. (1976) - *Rayleigh waves phase velocities and upper mantle structure in the Apennines*. Ann. Geof., **29**: 199-214.

CATALANO R., DI STEFANO P., SULLI A. & VITALE F.P. (1996) *Paleogeography and structure of the central Mediterranean: Sicily and its offshore area*. Tectonophysics, **260**: 291-323.

CATALANO R., DOGLIONI C. & MERLINI S. (2001) - *On the Mesozoic Ionian Basin*. Geophys. J. Int., **144**: 49-64.

CERNOBORI L., HIRN A., MCBRIDE J.H., NICOLICH R., PETRONIO L., ROMANELLI M. & STREAMERS/PROFILES WORKING GROUPS (1996) - *Crustal image of the Ionian basin and its Calabrian margin*. Tectonophysics, **264**: 175-189.

CHIMERA G., AOUDIA A., SARAO' A. & PANZA G.F. (2003) - *Active Tectonics in Central Italy: constraints from surface wave tomography and source moment tensor inversion*. Phys. Earth Planet. Inter., **138**: 241-262.

CINQUE A., CIVETTA L., ORSI G. & PECCERILLO A. (1988) - *Geology and geochemistry of the Island of Ustica (Southern Tyrrhenian Sea)*. Boll. Soc. Ital. Miner. Petrol., **43**: 987-1002.

CONTICELLI S. & PECCERILLO A. (1992) - *Petrology and geochemistry of potassic and ultrapotassic volcanism from Central Italy: inferences on its genesis and on the mantle source evolution*. Lithos, **28**: 221-240.

CONTICELLI S., D'ANTONIO M., PINARELLI L., CIVETTA L. (2001) - *Source contamination and mantle heterogeneity in the genesis of Italian potassic and ultrapotassic rocks: Sr-Nd-Pb isotope data from Roman Province and southern Tuscany*. Mineral. Petrol., **74**: 189-222.

CRISTOFOLINI R., GHISETTI F., SCARPA R. & MEZZANI L. (1985) - *Character of the stress field in the Calabrian Arc and Southern Apennines (Italy) as deduced by geological, seismological and volcanological information*. In: EVA, C. PAVONI, N (Eds.): *"Seismotectonics"*. TECTONOPHYSICS, **117**: 39-58.

CRISTOFOLINI R., MENZIES M.A., BECCALUVA L. & TINDLE A. (1987) - *Petrological notes on the 1983 lavas at Mount Etna, Sicily, with reference to their REE and Sr-Nd isotopic composition*. Bull. Volcanol., **49**: 599-607.

DE ASTIS G., PECCERILLO A., KEMPTON P.D., LA VOLPE L. & WU T.W. (2000) - *Transition from calcalkaline to potassium-rich magmatism in subduction environments: geochemical and Sr, Nd, Pb isotopic constraints from the Island of Vulcano (Aeolian arc)*. Contrib. Mineral. Petrol., **139**: 684-703.

DE FINO M., LA VOLPE L., PECCERILLO A., PICCARRETA G. & POLI G. (1986) - *Petrogenesis of Monte Vulture volcano (Italy): inferences from mineral chemistry, major and trace element data*. Contrib. Miner. Petrol., **92**: 135-145.

DE GORI P., CIMINI G.B., CHIARABBA C., DE NATALE G., TROISE C. & DESCHAMPS A. (2001) - *Teleseismic tomography of the Campanian volcanic area and surrounding Apenninic belt. J. Volc*. Geoth. Res., **109**: 55-75.

DEGROOT-HEDLIN C. & CONSTABLE S. (1990) - *Occam's inversion to generate smooth, two-dimensional models from magnetotelluric data*. Geophysics, **55**: 1613-1624.

DELLA VEDOVA B., PELLIS G. & PINNA E. (1989) - *Studio geofisico dell'area di transizione tra il Mar Pelagico e la piana abissale dello Ionio*. Atti 8° Convegno Annuale G.N.G.T.S., Roma, 543-558.

DELLA VEDOVA B., MARSON I., PANZA G.F. & SUHADOLC P. (1991) - *Upper mantle properties of the Tuscan-Tyrrhenian area: a framework for its recent tectonic evolution*. Tectonophysics, **195**: 311-318.

DE MATTEIS R., LATORRE D., ZOLLO A. & VIRIEUX J. (2000) - *1D P-velocity models of Mt. Vesuvio Volcano from the Inversion of TomoVes96 first arrival time data*. Pure Appl. Geophys., **157**: 1643-1661.

DE VOGGD B., TRUFFERT C., CHAMOT-ROOKE N., HUCHON P., LALLERMANT S. & LE PICHON X., (1992) - *Two-ship deep seismic soundings in the basins of the Eastern Mediterranean Sea (Pasiphae cruise)*. Geophys. J. Int., **109**: 536-552.

DI GIROLAMO P. (1978) - *Geotectonic setting of Miocene-Quaternary in and around the eastern Tyrrhenian Sea border (Italy) as deduced from major element geochemistry*. Bull. Volcanol., **41**: 229-250.

DITMAR P.G. & YANOVSKAYA T.B. (1987) - *A generalization of the Backus-Gilbert method for estimation of lateral variations of surface wave velocity*. Izv. AN SSSR, Fiz. Zemli (Physics of the Solid Earth), **23** (6): 470-477.

DOGLIONI C., HARABAGLIA P., MERLINI S., MONGELLI F., PECCERILLO A. & PIROMALLO C. (1999) - *Orogens and slabs vs. their direction of subduction*. Earth Sci. Review, **45**: 167-208.

DOGLIONI C., INNOCENTI F. & MARIOTTI G. (2001) - *Why Mt. Etna?* Terra Nova, **13**: 25-31.

DU Z.J., MICHELINI A. & PANZA G.F. (1998) - *EurID: a regionalised 3-D seismological model of Europe*. Phys. Earth Planet. Inter., **105**: 31-62.

FERRUCCI F., GAUDIOSI G., HIRN A. & NICOLICH R. (1991) - *Ionian Basin and Calabrian Arc: some new elements from DSS data*. Tectonophysics, **195**: 411-419.

FINETTI I. (1982) - *Structure, stratigraphy and evolution of central Mediterranean*. Boll. Geof. Teor. Appl., **24**: N. 96.

FINETTI I. & DEL BEN A. (1986) - *Geophysical study of the Tyrrhenian opening*. Boll. Geofis. Teor. Appl., **28**, 110: 75-156.

FINETTI I.R., BOCCALETTI M., BONINI M., DEL BEN A., GELETTI R., PIPAN M. & SANI F. (2001) - *Crustal section based on CROP seismic data across the North Tyrrhenian - Northern Apennines - Adriatic Sea*. Tectonophysics, **343**: 135-163.

FOLEY S.F. (1992) - *Vein-plus-wall-rock melting mechanisms in the lithosphere and the origin of potassic alkaline magmas*. Lithos, **28**: 435-453.

FOLEY S.F., VENTURELLI G., GREEN D.H. & TOSCANI L. (1987) - *The ultrapotassic rocks: characteristics, classification and constraints for petrogenesis*. Earth Sci. Rev., **24**: 81-134.

FRANCALANCI L., TOMMASINI S., CONTICELLI S. & (1999) - *Sr isotope evidence for short magma residence time for the 20th century activity at Stromboli volcano, Italy*. Earth and Planet. Sc. Lett., **167**, 1-2: 61-69.

FREZZOTTI ML., PECCERILLO A., BONELLI R. (2003) -

Magma ascent rates and depths of magma reservoirs beneath the Aeolian volcanic arc (Italy): inferences from fluid and melt inclusions in crustal xenoliths. In R.J. BODNAR & B. DE VIVO (Eds.): "*Melt inclusions in volcanic systems*". Elsevier, Amsterdam,185-206.

GAUTHIER P.J. & CONDOMINES M. (1999) *210Pb–226Ra radioactive disequilibria in recent lavas and radon degassing: inferences on the magma chamber dynamics at Stromboli and Merapi volcanoes*. Earth and Planet. Sc. Lett., **172**, 1-2: 111-126.

GRAHAM E.K. (1970) - *Elasticity and composition of the upper mantle*. Geophys. J. R. Astr. Soc., **20**: 285-302.

IMPROTA L., IANNACCONE G., CAPUANO P., ZOLLO A. & SCANDONE P. (2000) - *Inferences on the upper crustal structure of Southern Apennines (Italy) from seismic refraction investigations and surface data*. Tectonophysics, **317**: 273-297.

KERN H. & SCHENK V. (1988) - *A model of velocity structure beneath Calabria, southern Italy, based on laboratory data*. Earth and Planet. Sc. Lett., **87**: 325-337.

KNOPOFF L. (1972) - *Observations and inversion of surface-wave dispersion*. In: RITSEMA A.R. (Ed.): "*The Upper Mantle*". Tectonophysics, **13** (1-4): 497-519.

KNOPOFF L. & PANZA G.F. (1977) - *Resolution of Upper Mantle Structure using higher modes of Rayleigh waves*. Annales Geophysicae, **30**: 491-505.

LOCARDI E. (1986) - *Tyrrhenian volcanic arcs: volcano-tectonics, petrogenesis and economic aspects*. In: F.C. WEZEL (Ed.): "*The origin of the arcs*". Elsevier, 351-373.

LOCARDI E. (1988) - *The origin of the Apenninic arc*. In: WEZEL, F.C. (Ed.): "*The Origin and Evolution of the Arcs*". Tectonophysics, **146**: 105-123.

LOCARDI E. (1993) - *Dynamics of deep structures in the Tyrrhenian-Apennines area and its relation to neotectonics*. Il Quaternario, **6**: 59-66.

LOCARDI E. & NICOLICH R. (1988) - *Geodinamica del Tirreno e dell'Appennino centro-meridionale: la nuova carta della Moho*. Mem. Soc. Geol. It., **41**: 121-140.

LUDWIG W.J., NAFE J.E., DRAKE C.L. (1970) - *Seismic refraction*. In: WILEY-INTERSCI. *The Sea*, New York. Vol. 4, Part 1: 53-84.

MANTOVANI E., NOLET G. & PANZA G.F. (1985) - *Lateral heterogeneity in the crust of the Italian region from regionalized Rayleigh-wave group velocities*. Annales Geophysicae, **3**: 519-530.

MARSON I., PANZA G.F. & SUHADOLC P. (1995) - *Crust and upper mantle models along the active Tyrrhenian rim*. Terra Nova, **7**: 348-357.

MCNUTT M.K. (1998) - *Superswells*, Rev. Geophys. **36**: 211-244.

MELETTI C., PATACCA E. & SCANDONE P. (2000) - *Construction of a Seismotectonic Model: The Case of Italy*. Pure Appl. Geophys., **157**: 11-35.

MORELLI C. (1998) - *Lithospheric structure and geodynamics of the Italian peninsula derived from geophysical data: a review*. Mem. Soc. Geol. It., **52**: 113-122.

MOSTAANPOUR M.M. (1984) - Einheitliche Auswertung krustenseismicher daten in Westeuropa. Darstellung von Krustenparametern und Laufzeitanomalien. Verlag von Dirtrich Reimer in Berlin.

PANZA G.F. (1980) - *Evolution of the Earth's lithosphere. NATO Adv. Stud. Inst. Newcastle, 1979*. In: DAVIES P.A. & RUNCORN S.K. (Eds.): "*Mechanisms of Continental Drift and Plate Tectonics*". Academic Press: 75-87.

PANZA G.F. (1981) - *The resolving power of seismic surface waves with respect to crust and upper mantle structural models*. In: CASSINIS R. (Ed.): "*The solution of the inverse problem in geophysical interpretation*". Plenum Publ. Corp.: 39-77.

PANZA G.F. (1984) *Contributi geofisici alla geologia: stato attuale dell'arte e prospettive future*. In: "*Cento anni di geologia italiana*". Vol. giub. I Centenario S.G.I., 363-376, Bologna.

PANZA G.F., CALCAGNILE G., SCANDONE P. & MUELLER S. (1980) - *La struttura profonda dell'area mediterranea*. Le Scienze, **141**: 60-69.

PANZA G.F., PONTEVIVO A., CHIMERA G., RAYKOVA R. & AOUDIA A. (2003) - *The lithosphere-asthenosphere: Italy and surroundings*. Episodes, **26**: 169-174.

PASYANOS M.E., WALTER W.R. & HAZLER S.E. (2001) - *A surface wave dispersion study of the Middle East and North Africa for Monitoring the Compressive Nuclear-Test-Ban Treaty*. Pure Appl. Geophys., 158: 1445-1474.

PECCERILLO A. (1999) - *Multiple mantle metasomatism in central-southern Italy: geochemical effects, timing and geodynamic implications*. Geology, **27**: 315-318.

PECCERILLO A. (2001a) - *Geochemistry of Quaternary magmatism in central-southern Italy: genesis of primary melts and interaction with crustal rocks*. Geochemistry International, **39**: 521-535.

PECCERILLO A. (2001b) - *Geochemical affinities between Vesuvius, Phlegraean Fields and Stromboli volcanoes: petrogenetic, geodynamic and volcanological implications*. Mineral. Petrol., **73**: 93-105.

PECCERILLO A. & PANZA G.F. (1999) - *Upper mantle domains beneath Central-Southern Italy: petrological, geochemical and geophysical constraints*. Pure Appl. Geophys., **156**: 421-443.

PECCERILLO A., POLI G. & SERRI G. (1988) - *Petrogenesis of orenditic and kamafugitic rocks from Central Italy*. Canad. Mineral., **26**: 45-65.

PEPE F., BERTOTTI G., CELLA F. & MARSELLA E. (2000) - *Rifted margin formation in the south Tyrrhenian Sea: a high-resolution seismic profile across the north Sicily passive continental margin*. Tectonics, **19**, 2: 241-257.

PIALLI G., ALVAREZ W. & MINELLI G. (1995) - *Geodinamica dell'Appennino settentrionale e sue ripercussioni nella evoluzione tettonica miocenica*. Studi geol. Camerti, Volume speciale 1995/1: 523-536.

POLI G., FREY F.A. & FERRARA G. (1984) - *Geochemical characteristics of the south Tuscany (Italy) volcanic province: constraints on lava petrogenesis*. Chem. Geol., **43**: 203-221.

PONTEVIVO A. & PANZA G.F. (2002) - *Group Velocity Tomography and Regionalization in Italy and bordering areas*. Phys. Earth Planet. Inter., **134**: 1-15.

RINGWOOD A.E. (1966) - *Mineralogy of the mantle*. In: P.M. HURLEY (Ed.): "*Advances in Earth Science*". MIT Press, 357-399.

SCARASCIA S. & CASSINIS R. (1992) - *Profili sismici a grande angolo esplorati in prossimità del tracciato del profilo Crop01: una raccolta dei risultati e qualche revisione*. Studi geol. Camerti, volume speciale CROP 1-1A: 17-26.

SCARASCIA S., LOZEJ A. & CASSINIS R. (1994) - *Crustal structures of the Ligurian, Tyrrhenian and Ionian Seas and adjacent onshore areas interpreted from wide-angle seismic profiles*. Boll. Geof. Teor. Appl., **36**: 141-144.

TRUA T., SERRI G., MARANI M.P., RENZULLI A. & GAMBERI F. (2002) - *Volcanological and petrological evolution of Marsili Seamount (Southern Tyrrhenian Sea)*. J. Volcanol. Geotherm. Res., **114**: 441-464.

VALYUS V.P. (1972) - *Determining seismic profiles from a set of observations*. In: KEILIS-BOROK (Ed.): "*Computational Seismology*". Consult. Bureau, New-York: 114-118.

VALYUS V.P., KEILIS-BOROK V.I. & LEVSHIN A. (1969) - *Determination of the upper-mantle velocity cross-section for Europe*. Proc. Acad. Sci. USSR, **185**, 3.

VENISTI N., CALCAGNILE G., PONTEVIVO A. & PANZA G.F.

(2003) - *Surface wave and body wave tomography combined study of the Apulian Plate*. Submitted to PAGEOPH.

WENDLANDT R.F. & EGGLER D.H. (1980) - *The origin of potassic magmas: stability of phlogopite in natural spinel lherzolite an in the KAlSiO4-MgO-SiO2-H2O-CO2 at high pressures and high temperatures*. Amer. J. Sci., **280**: 421-458.

YANOVSKAYA T.B. & DITMAR P.G. (1990) - *Smoothness criteria in surface-wave tomography*. Geophys. J. Int., **102**: 63-72.

ZANON V., FREZZOTTI M. & PECCERILLO (2003) - *Magmatic feeding system and crustal magma accumulation beneath Vulcano Island (Italy): evidence from CO2 fluid inclusions in quartz xenoliths* . Geophys. J. Res., **108**, B6, In press.